J. Fluid Mech. (1990), *vol.* 210, *pp.* 593–626
Printed in Great Britain

On the Lagrangian description of unsteady boundary-layer separation. Part 1. General theory

By LEON L. VAN DOMMELEN[1] AND STEPHEN J. COWLEY[2]

[1] Department of Mechanical Engineering, FAMU/FSU College of Engineering, PO Box 2175, Tallahassee, FL 32316-2175, USA

[2] Department of Mathematics, Imperial College of Science, Technology and Medicine, Huxley Building, 180 Queen's Gate, London SW7 2BZ, UK

(Received 27 May 1983 and in revised form 3 July 1989)

Although unsteady, high-Reynolds-number, laminar boundary layers have conventionally been studied in terms of Eulerian coordinates, a Lagrangian approach may have significant analytical and computational advantages. In Lagrangian coordinates the classical boundary-layer equations decouple into a momentum equation for the motion parallel to the boundary, and a hyperbolic continuity equation (essentially a conserved Jacobian) for the motion normal to the boundary. The momentum equations, plus the energy equation if the flow is compressible, can be solved independently of the continuity equation. Unsteady separation occurs when the continuity equation becomes singular as a result of touching characteristics, the condition for which can be expressed in terms of the solution of the momentum equations. The solutions to the momentum and energy equations remain regular. Asymptotic structures for a number of unsteady three-dimensional separating flows follow and depend on the symmetry properties of the flow (e.g. line symmetry, axial symmetry). In the absence of any symmetry, the singularity structure just prior to separation is found to be quasi two-dimensional with a displacement thickness in the form of a crescent-shaped ridge. Physically the singularities can be understood in terms of the behaviour of a fluid element inside the boundary layer which contracts in a direction parallel to the boundary and expands normal to it, thus forcing the fluid above it to be ejected from the boundary layer.

1. Introduction

A major feature of unsteady large-Reynolds-number flow past a rigid body is the shedding of vortices from the surface of the body. Such vortices alter the forces exerted on the body dramatically (McCroskey & Pucci 1982). A more complete theoretical understanding of vortex shedding would be advantageous in the design of air, land and water transport. Theoretical models of vortex shedding also have application, *inter alia*, in the description of air flow over hills and water waves, water flow over sand ripples, and blood flow through curved and constricted arteries and veins.

A classical example of vortex shedding develops when a circular cylinder is set into motion in the direction normal to its axis. This example was first studied by Prandtl (1904), and the process by which an initially attached boundary layer develops into a separated flow with detached free shear layers has been clearly illustrated by the experiments of Nagata, Minami & Murata (1979), and Bouard & Coutanceau (1980). The term 'separation' will in this paper be used to refer to the 'breakaway' of a thin

layer of vorticity from the surface of a body. This definition of separation is close to that of both Prandtl (1904) and Sears & Telionis (1975). In particular, Sears & Telionis speak only of separation when the penetration of the boundary-layer vorticity away from the wall becomes too large to be described on the usual $O(Re^{-\frac{1}{2}})$ boundary-layer scale (Re is the Reynolds number of the flow, and is assumed large). Therefore, once separation has developed the classical attached flow solution will, in general, no longer be valid.

The first theoretical advance in understanding the unsteady cylinder flow at high Reynolds numbers was made by Blasius (1908). He explained the occurrence of flow reversal inside the attached unsteady boundary layer which is set up immediately the cylinder starts to move. In the case of steady flow past a rigid surface, flow reversal is often accompanied by separation. However, Moore (1958), Rott (1956) and Sears (1956) all realized that zero wall shear is not necessarily related to separation in unsteady flow. Sears & Telionis (1975) noted subsequently that their definition of separation is consistent with the termination of the boundary-layer solution in a singularity. Such a singularity will be referred to as the separation singularity, and the time at which it develops as the separation time.

A considerable number of numerical computations have attempted to verify the existence of a singularity in the boundary-layer solution for the circular cylinder problem. The first convincing evidence that a singularity forms within a finite time was given by Van Dommelen & Shen (1977, 1980*a*, 1982). In a Lagrangian computation, with fluid particles as independent coordinates, they found that a separation singularity develops after the cylinder has moved approximately $\frac{3}{4}$ of a diameter. The existence of this singularity has been confirmed by the finite-difference numerical calculations of Ingham (1984) and Cebeci (1982) (however see Cebeci 1986), and the computer extended series solution of Cowley (1983). These calculations were all based on Eulerian formulations. A similar two-dimensional separation singularity has been observed using Lagrangian procedures on an impulsively started ellipse at several angles of attack (L. L. Van Dommelen, T. Wu, C. Chen & S. F. Shen, unpublished results), on pitching cylinders (Shen & Wu 1988; Wu 1989), in vortex-induced separation and turbulence production (Walker 1988), on an impulsively started sphere (Van Dommelen 1987), and using Eulerian schemes in leading-edge stall (Cebeci, Khattab & Schimke 1983) and about a rotating cylinder (Ece, Walker & Smith 1984).

Apart from vortex methods, flows with free surfaces, and some more specialized compressible flow computations, Lagrangian coordinates have not been as widely used as their Eulerian counterparts in fluid mechanics, especially for boundary-layer flows. Yet for some flows, such as unsteady flows in which advection dominates diffusion, Lagrangian coordinates seem more appropriate (e.g. see the inviscid calculations of Stern & Paldor 1983; Russel & Landahl 1984 and Stuart 1988). As far as unsteady separation is concerned, the advantage of a Lagrangian approach stems from the fact that in these coordinates the classical boundary-layer equations decouple into a momentum equation for the motion parallel to the boundary, and a continuity equation for the motion normal to the boundary (Shen 1978*a*, *b*). The solution of the former equation can be found independently of the latter. Moreover, while the time that the separation singularity develops can be identified from the solution to the momentum equation, only the solution to the continuity equation is singular (see §2).

An important consequence of the Lagrangian approach is that simple descriptions can be found to a wide variety of separations in one-, two- and three-dimensional

unsteady flows. In this paper we consider unsteady flows in general, then in Part 2 (Van Dommelen 1989) the separation process that occurs at the equatorial plane of a sphere which is set into a spinning motion is examined in detail.

In the next section we develop the simple analytic machinery needed to find self-consistent three-dimensional separation structures for both compressible and incompressible fluids. Some of the properties of the Lagrangian version of the boundary-layer equations are also discussed. In §3 the Lagrangian structure for three-dimensional separation is derived under the assumption that the flow can be completely general, then in §4 the changes in structure are discussed when various symmetries restrict the flow geometry.

2. Lagrangian formulation

The Lagrangian description of boundary-layer flow uses fluid particles (i.e. infinitesimal masses of fluid) as the basis of the coordinate system. A convenient coordinate system for the fluid particles (ξ, η, ζ) is given by the initial Eulerian position of the particles (see Lamb 1945 for example):

$$\xi \equiv (\xi, \eta, \zeta) = (x, y, z) \quad \text{at} \quad t = 0. \tag{2.1}$$

The precise form of the Lagrangian solution depends on the particular reference time, defined here as the start of the motion, but the physical solution is independent of it.

Following Rosenhead (1963) we assume that the position coordinates x and z describe an orthogonal coordinate system on the surface of the body in question. The lengths of the line elements $\mathrm{d}x$ and $\mathrm{d}z$ are taken as $h_1\,\mathrm{d}x$ and $h_3\,\mathrm{d}z$ respectively. The coordinate normal to the surface is denoted by y, which is scaled with the square root of the reference shear viscosity.

In Lagrangian coordinates, conservation of volume for a compressible fluid can be expressed in terms of a Jacobian determinant as follows (e.g. Hudson 1980):

$$\rho H(x,z)\, J(x,y,z) = \rho_0 H_0, \tag{2.2a}$$

where

$$J(x,y,z) = \begin{vmatrix} x_{,\xi} & x_{,\eta} & x_{,\zeta} \\ y_{,\xi} & y_{,\eta} & y_{,\zeta} \\ z_{,\xi} & z_{,\eta} & z_{,\zeta} \end{vmatrix}, \quad \rho_0(\xi,\eta,\zeta) = \rho(\xi,\eta,\zeta,0), \tag{2.2b, c}$$

$$H(x,z) = h_1(x,z)\, h_3(x,z), \quad H_0 = H(\xi,\zeta), \tag{2.2d, e}$$

$\rho(\xi, \eta, \zeta, t)$ is the density of the fluid, and a subscript comma denotes a Lagrangian derivative. The velocity components of the flow are related to the fluxions of position by

$$u = h_1(x,z)\,\dot{x}, \quad w = h_3(x,z)\,\dot{z}, \tag{2.3a, b}$$

where a dot represents a Lagrangian time derivative.

For compressible flow, the momentum and energy equations are (e.g. Rosenhead 1963):

$$\rho\left(\dot{u} + (uh_{1z} - wh_{3x})\frac{w}{H}\right) = -\frac{1}{h_1}p_x + \mathrm{D}_y(\mu \mathrm{D}_y u) + \rho g_x, \tag{2.3c}$$

$$\rho\left(\dot{w} + (wh_{3x} - uh_{1z})\frac{u}{H}\right) = -\frac{1}{h_3}p_z + \mathrm{D}_y(\mu \mathrm{D}_y w) + \rho g_z, \tag{2.3d}$$

$$\rho\frac{\partial e}{\partial \rho}\dot{\rho} + \rho\frac{\partial e}{\partial p}\dot{p} - \frac{p}{\rho}\dot{\rho} = \mu((\mathrm{D}_y u)^2 + (\mathrm{D}_y w)^2) + \mathrm{D}_y\left(\frac{\mu}{\sigma}\mathrm{D}_y T\right), \tag{2.3e}$$

where μ is the scaled shear viscosity, σ is the Prandtl number, and g_x and g_z are the components of the acceleration of gravity. The temperature, T, and internal energy, e, are assumed to be functions of density and pressure, while the pressure, p, is a known function of x, z and t; thus

$$\dot{p} = p_t + \frac{u}{h_1} p_x + \frac{w}{h_3} p_z. \tag{2.3f}$$

For an incompressible flow $\dot{\rho} = 0$ and e is taken to be a function of T and p.

Although the y-derivative D_y is Eulerian in nature, it can be written in the Lagrangian form (see also Shen 1978 *a*, *b*):

$$\mathrm{D}_y u = \frac{\rho(\xi, \eta, \zeta, t) H(x, z) J(x, u, z)}{\rho_0(\xi, \eta, \zeta) H(\xi, \zeta)}. \tag{2.4}$$

From (2.4) it follows that at a fixed wall the Eulerian D_y and Lagrangian $\partial/\partial\eta$ operators differ only by the density ratio, which leads to simplifications in the calculation of the wall shear.

If the boundary can move, appropriate boundary conditions to (2.3) are

$$(u, w, \rho) = (u_\mathrm{b}(x, z, t), w_\mathrm{b}(x, z, t), \rho_\mathrm{b}(x, z, t)) \quad \text{on} \quad y = 0, \tag{2.5a}$$

$$(u, w, \rho) \to (u_\mathrm{e}(x, z, t), w_\mathrm{e}(x, z, t), \rho_\mathrm{e}(x, z, t)) \quad \text{as} \quad y \to \infty, \tag{2.5b}$$

where u_b and w_b specify the velocity of the boundary in the x- and z-directions respectively, u_e and w_e are the corresponding external slip-velocities, ρ_e is the external flow density, and the wall density ρ_b can be given implicitly as the temperature at the wall. Ordinarily, these boundary conditions translate immediately to the Lagrangian domain by means of (2.3*a*, *b*). In the case of suction or blowing through the wall, they must be applied at an η-boundary moving through the Lagrangian domain; however, the wall boundary conditions turn out to be of little importance for the local analysis of this paper.

The principle advantages of Lagrangian coordinates derive from the absence of both the normal particle position y and the normal velocity component v from (2.3) and (2.4). Consequently, the particles' motion, as projected onto the surface of the body (x, z), can be found independently of the normal particle position y. Subsequent integration of the Jacobian (2.2) along lines of particles at constant projected position (x, z) yields the normal particle position

$$y = \int_0^s \frac{\rho_0 H_0 \, \mathrm{d}s}{\rho H |\nabla x \wedge \nabla z|}, \tag{2.6}$$

where $\mathrm{d}s^2 = \mathrm{d}\xi^2 + \mathrm{d}\eta^2 + \mathrm{d}\zeta^2$, $\nabla x = (x_{,\xi}, x_{,\eta}, x_{,\zeta})$ is the Lagrangian gradient, and the integral is performed in the Lagrangian $(\xi, \eta, \zeta; t)$ coordinate system along the lines of constant x, z, and t, i.e. lines which in physical space are vertical through the boundary layer.

The central issue of this paper can now be stated: we hypothesize that during the evolution toward separation, the projected position (x, z) can remain regular, and commonly does remain regular. When true, such regularity strongly restricts the possible behaviour of x and z near separation, and to characterize separation we need only identify the nature of solutions to the continuity equation (2.2) or (2.6) – an equation which is much simpler than the momentum equations. The remaining ambiguity in the behaviour of x and z is resolved using arguments of symmetry.

Various arguments to justify our hypothesis can be given. One of them is self-consistency. If it is assumed that x, z, u, w, and ρ are non-singular at the separation

time t_s, then the solution to the Lagrangian momentum equations can be expanded in powers of $(t-t_s)$ to any algebraic order. In contrast, the usual Eulerian asymptotic expansions show only that the first few terms in the expansions are self-consistent.

As another argument, Van Dommelen (1981) showed analytically that the *inviscid* incompressible two-dimensional equations have solutions, x, z, which are regular functions of the Lagrangian variables, although $y(\xi, t)$ is singular (this analysis can be further developed by expanding in powers of a small coefficient of viscosity). Yet this example is somewhat artificial; physically it would require that during the evolution of the boundary layer the coefficient of viscosity was changed significantly by some external means.

A more powerful argument is possibly the capability of the analysis in this paper to reproduce and extend several known separation processes previously analysed in Eulerian coordinates. However, the most convincing argument is provided by actual numerical solutions of the Lagrangian boundary-layer equations. For example, Van Dommelen & Shen's (1980*a*) computation of the boundary layer on an impulsively started circular cylinder provided direct numerical evidence as to regularity of the momentum equation. Further, it is in remarkably close agreement with the results obtained by Cowley (1983) using a series extension technique. In particular, Cowley (1983) finds a singularity in the solution at the same time and position as the Lagrangian computations. Ingham (1984) performed an Eulerian Fourier series expansion of the solution in the direction along the cylinder. By carefully increasing the order of expansion as the spectrum expands due to the incipient singularity, he obtained results in close agreement with those of both Van Dommelen & Shen (1980*a*) and Cowley (1983). The fact that these three very different procedures were found to produce results in excellent agreement with one another until very close to the breakdown of the solution at separation is reassuring, since a number of more conventional finite-difference computations (e.g. Telionis & Tsahalis 1974; Wang 1979; Cebeci 1986) give significantly different results. The finite-difference results of Henkes & Veldman (1987) are exceptions because they remain in agreement with the three unconventional methods until relatively close to the singularity (although they disagree with Cebeci (1986) at a significantly earlier time). One of the difficulties with conventional finite-difference procedures, as pointed out by Cebeci (1986), is the need to satisfy the CFL condition, a condition which is implicitly satisfied by the three procedures of Van Dommelen & Shen, Cowley and Ingham. (See also the integral method of Matsushita, Murata & Akamatsu 1984.)

Clearly in any numerical Lagrangian computations, it is not possible to *prove* that the solution is regular, since the inevitable upper limit on resolution means that high-order singularities are difficult to resolve. However, in the accompanying numerical study, Part 2, the boundary layer at the equatorial plane of a spinning sphere is solved using up to 1000 mesh points across the boundary layer. Even at such high resolution, no trace of singular behaviour was observed, and derivatives of high order could be evaluated precisely.

When the fact that solutions to the momentum equations are regular is accepted, (and for compressible flow in addition the density must be regular), the next question to arise is what implications such regularity has for the structure of the separation process. First, only the continuity equation can develop singular behaviour, and from (2.2) or (2.6) it follows that this is only possible if the Lagrangian gradients of x and z become parallel, i.e. if at some point s

$$\nabla x = \lambda_s \nabla z, \tag{2.7a}$$

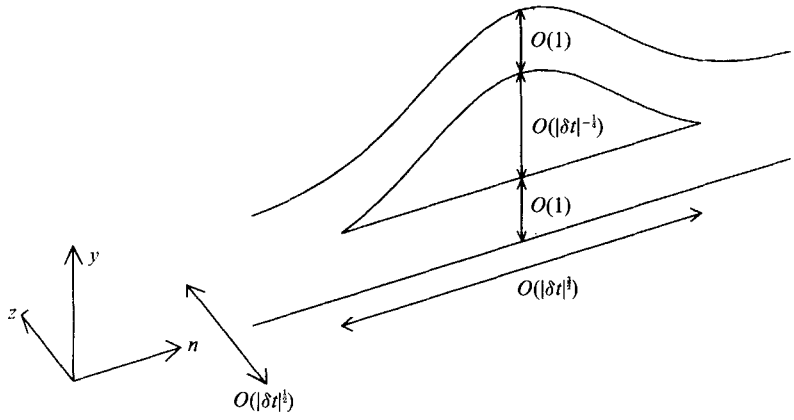

FIGURE 1. Structure of the separating boundary layer, illustrating the asymptotic scalings in the boundary-layer coordinate system (schematic).

where λ_s is a constant (Shen 1978*b*). Generally, the point s of interest is the particle and time at which (2.7*a*) is satisfied for the first time. The condition (2.7*a*) is a three-dimensional extension of the two-dimensional condition pointed out by Van Dommelen & Shen (1980*a*); it requires that a Lagrangian stationary point, $\nabla n = 0$, exists for an oblique coordinate

$$n = x - \lambda_s z. \tag{2.7b}$$

An alternative way to phrase the condition for singular y is to define a unit vector in the n-direction tangential to the wall,

$$\boldsymbol{n} = (n_x, n_z) = \frac{h_x h_z}{(h_z^2 + h_x^2 \lambda_s^2)^{\frac{1}{2}}} \left(\frac{1}{h_x}, -\frac{\lambda_s}{h_z} \right). \tag{2.7c}$$

A singularity occurs when, for all infinitesimal changes $\partial\boldsymbol{\xi}$ in fluid particle, the corresponding changes $\partial\boldsymbol{r}$ in particle position satisfy

$$\boldsymbol{n} \cdot \partial\boldsymbol{r} = 0, \quad \partial\boldsymbol{r} = (h_x \partial x, h_z \partial z). \tag{2.7d, e}$$

This implies that an infinitesimal particle volume $\partial\xi\,\partial\eta\,\partial\zeta$ around point s has been compressed to zero physical size in the n-direction. But since particle volume (or mass in compressible flow) is conserved, the compression in the n-direction along the wall is compensated for by a rapid expansion in the y-direction which drives the fluid above the compressed region $\partial\xi\,\partial\eta\,\partial\zeta$ 'far' from the wall to form a separating vorticity layer.

In this paper asymptotic expansions will be derived when the difference in time δt from the time that the first singularity occurs is small, so that the boundary layer is close to separation (but not yet interactive). That implies that (2.7*a*) is nearly satisfied and the boundary-layer thickness is large. For the non-degenerate three-dimensional case analysed in §3, in the Eulerian (n, y)-plane through the particle s the boundary layer assumes a structure as sketched in figure 1. The streamwise lengthscale for the relevant 'inner' expansion around the point s turns out to be small of order $|\delta t|^{\frac{3}{2}}$. The vertical scale is large compared to the $Re^{-\frac{1}{2}}$ transverse boundary-layer scale; this scale is physically proportional to $|\delta t|^{-\frac{1}{4}} Re^{-\frac{1}{2}}$. The vertically expanding region propels a layer of vorticity carrying boundary-layer fluid above it away from the wall. The 'ejected' layer retains a typical thickness proportional to

$Re^{-\frac{1}{2}}$. The variations in the z-direction out of the (n, y)-plane are much slower than those in the plane, and the structure assumes a quasi-two-dimensional form.

From (2.6) it can be shown that the above vertical expansion process constitutes separation in the sense of Sears & Telionis (1975), since the particle distance from the wall becomes too large, 'infinite', to be described on the usual boundary-layer scale. Note that the assumed regularity of x and z does not allow an infinite expansion in the direction parallel to the wall but normal to $\boldsymbol{n}$; the particle can only expand strongly in the direction away from the wall. Similarly for a compressible fluid, the assumed regularity of ρ is inconsistent with an infinite compression of the particle volume. (At present there is no direct numerical evidence for the regularity assumption in the compressible case, although it is of course self-consistent.)

From (2.7) we can derive generalized so-called Moore–Rott–Sears (MRS) conditions at the stationary point, similar to the conditions formulated by Sears & Telionis (1975) for two-dimensional flow. The form of the Eulerian D_y operator (2.4) implies using (2.2*b*) and (2.7*a*) that the vorticity vanishes at that point, i.e.

$$\mathrm{D}_y u = \mathrm{D}_y w = 0 \quad \text{at} \quad \nabla n = 0. \tag{2.8a}$$

In fact, the D_y operator vanishes for all quantities which remain regular in the Lagrangian domain.

The second MRS condition is more complicated. Since (2.7*a*) is equivalent to two conditions on the Lagrangian derivatives of x and z, in three-dimensional space we expect it to be satisfied on a curve of particles for times beyond the first occurrence of separation (cf. §§3 and 4.3). The Eulerian projection of the singular curve on the wall will be denoted by $\boldsymbol{x}_{\mathrm{MRS}} = (x_{\mathrm{MRS}}, z_{\mathrm{MRS}})$ and differential changes in the physical position of this curve by $\mathrm{d}\boldsymbol{r}_{\mathrm{MRS}} = (h_x \mathrm{d}x_{\mathrm{MRS}}, h_z \mathrm{d}z_{\mathrm{MRS}})$. The second MRS condition concerns the motion of this projected curve. To derive it, we focus attention on an arbitrary point s on the singular curve (rather than our usual choice in which s is the first point at which a singularity occurs). First we consider a Lagrangian differential $\partial\xi$ along the singular curve passing through point s, keeping time constant. Since x and z are functions of ξ and t only, $\partial\xi$ corresponds to a change in Eulerian position along the projected curve which satisfies (2.7*d*),

$$\boldsymbol{n} \cdot \partial \boldsymbol{r}_{\mathrm{MRS}} = 0, \tag{2.8b}$$

so that the singular curve is normal to the local vector $\boldsymbol{n}$. As for any curve, the propagation velocity of this curve is given by the component of the propagation velocity of points on the curve in the direction normal to the curve. To find an expression for it, we now consider a total differential in Lagrangian space–time at the point s, resulting in changes $\mathrm{d}x_{\mathrm{MRS}} = \partial x_{\mathrm{MRS}} + \dot{x}_{\mathrm{s}} \mathrm{d}t$ and $\mathrm{d}z_{\mathrm{MRS}} = \partial z_{\mathrm{MRS}} + \dot{z}_{\mathrm{s}} \mathrm{d}t$. Since $(h_x \partial x_{\mathrm{MRS}}, h_z \partial z_{\mathrm{MRS}})$ satisfies (2.8*b*),

$$\boldsymbol{n} \cdot \frac{\mathrm{d}\boldsymbol{r}_{\mathrm{MRS}}}{\mathrm{d}t} = \boldsymbol{n} \cdot \boldsymbol{u}_{\mathrm{MRS}}, \quad \boldsymbol{u}_{\mathrm{MRS}} = (h_x \dot{x}_{\mathrm{s}}, h_z \dot{z}_{\mathrm{s}}), \tag{2.8c, d}$$

which shows that the propagation velocity of the singular curve equals the flow velocity of the singular particle s at the considered position $(x_{\mathrm{MRS}}, z_{\mathrm{MRS}})$.

While this three-dimensional form of the MRS conditions seems new, the general applicability of the two-dimensional case is fairly well established both theoretically (Moore 1958; Sears & Telionis 1975; Williams 1977; Shen 1978*a*; Sychev 1979, 1980; Van Dommelen & Shen 1980*b*, 1982, 1983*a*, *b*; Van Dommelen 1981) and experimentally (Ludwig 1964; Didden & Ho 1985).

The conditions derived seem consistent with the results of Williams (1978) for

unsteady three-dimensional boundary layers equivalent to steady, semi-similar flows over moving walls. In particular Williams found that in the steady-flow coordinate system, the velocity component normal to the separation line vanishes, which agrees with (2.8*c*) for a steady separation line. The profiles of one velocity component show a minimum and those of the other component an inflection point in apparent agreement with (2.8*a*). However, the inflection point has not yet fully achieved zero slope at the last position where the computation converged.

We can also verify the notion of Sears & Telionis (1975) that unsteady separation occurs in the middle of the boundary layer rather than at the wall. In the absence of a transpiration velocity, the motion of points on the wall equals the motion of the boundary-layer particles at the wall, cf. (2.5) and (2.3*a*, *b*). Thus a fluid particle at the wall can only contract to vanishing size in the n-direction if the wall itself performs the same contraction, which is not possible for a solid wall.

In the next sections the nature of the separation process is analysed. First we form local Taylor series expansions for the regular solutions to the momentum equations near the stationary point, and then we expand the solutions of the continuity equation in an asymptotic series. This procedure is similar to the one followed by Van Dommelen & Shen (1982) for two-dimensional separation. In contrast to the steady viscous singularities of Goldstein (1948) and Brown (1965), and the ideas of Sears & Telionis (1975), the unsteady singularity is essentially inviscid in character and consists of two vortex sheets separated by an increasingly large central inviscid region (as found by Ockendon (1972) for a rotating disc with suction, and by Sychev (1979, 1980), Van Dommelen & Shen (1980*b*, 1983*a*, *b*), Williams & Stewartson (1983) and Elliott, Cowley & Smith (1983) for steady separation over up- and downstream-moving walls). The leading-order asymptotic structure of the unsteady singularity has also been recovered by Van Dommelen (1981) as a matched asymptotic solution to the Eulerian boundary-layer equations. More generally, Elliott *et al.* (1983) showed that there is a certain amount of arbitrariness in the Eulerian expansions. The Lagrangian expansion resolves such arbitrariness by the assumption (supported by various numerical data, see Van Dommelen & Shen 1982, the closing remarks of §4.3, and Part 2) that the leading-order coefficients in the Taylor series expansion near the stationary point are non-zero.

3. Three-dimensional separation singularities

In this section we find the leading-order term of an asymptotic analysis which describes the local structure of the flow as unsteady separation is approached. The time and position at which the separation singularity first develops will be denoted by the subscript s; thus, for example

$$(\nabla n)_{\mathrm{s}} = 0, \tag{3.1a}$$

where n is the oblique coordinate corresponding to the initial separation, defined in (2.7*b*) as

$$n = x - \lambda_{\mathrm{s}} z. \tag{3.1b}$$

Note that the definition of the x- and z-coordinates can simply be interchanged if n and z are not independent coordinates. In index notation, (3.1*a*) can be written as $n_i = 0$, where we will adopt the convention to omit the subscripts comma (to indicate Lagrangian derivatives) and s (to indicate the separation particle at the separation time) if they occur together (i.e. $n_i = (n_{,t})_{\mathrm{s}}$).

The solution of the continuity equation (2.2) for y can be greatly simplified by a number of coordinate transformations for both the particle position coordinates (x, z) and the Lagrangian coordinates (ξ, η, ζ). Here we will select transformations which preserve the Jacobian J (2.2*b*), since these are algebraically more simple than transformations which preserve the physical volume HJ, or mass ρHJ.

As a first transformation, we drop the position coordinate x in favour of n, shift the Lagrangian coordinate system to the separation particle s, and rotate it, resulting in the set of coordinates

$$n = x - \lambda_s z, \quad z, \quad k_i = \sum_{j=1}^{3} a_{ij}(\xi_j - \xi_{js}), \tag{3.2a–c}$$

where $(\xi_1, \xi_2, \xi_3) = (\xi, \eta, \zeta)$ and a_{ij} is an orthonormal rotation matrix which is chosen to eliminate the mixed derivatives n_{12}, n_{13}, and n_{23}. Therefore, expanding n and z in a Taylor series expansion about the separation point, we obtain

$$n = n_s + \sum_{i=1}^{3} \tfrac{1}{2} n_{ii} k_i^2 + \ldots + \delta t \left(\dot{n}_s + \sum_{i=1}^{3} \dot{n}_i k_i + \ldots \right) + \ldots, \tag{3.3a}$$

$$z = z_s + \sum_{i=1}^{3} z_i k_i + \ldots + \delta t \dot{z}_s + \ldots, \tag{3.3b}$$

where $\delta t = t - t_s$ and the indices indicate differentiation with respect to the current Lagrangian coordinate system (k_1, k_2, k_3).

However, if t_s is the first time that a stationary point occurs, the Taylor series coefficients in (3.3) cannot be completely arbitrary: the singularity condition may not be satisfied anywhere for $\delta t < 0$. The condition for a singularity to exist for earlier times at some neighbouring point is, in terms of n and z,

$$n_{,i} - (\lambda - \lambda_s) z_{,i} = 0, \tag{3.4a}$$

where λ is the ratio between ∇z and ∇x at the neighbouring singular point. If we expand (3.4*a*) in a Taylor series, we obtain

$$n_{ii} k_i - z_i \delta\lambda + \dot{n}_i \delta t + \ldots = 0 \quad \text{for} \quad i = 1, 2, 3, \tag{3.4b}$$

where $\delta\lambda = \lambda - \lambda_s$. If all three coefficients n_{11}, n_{22}, and n_{33} were non-zero, (3.4*b*) would have leading-order solutions for any $\delta t < 0$. These leading-order solutions can be iterated to solutions of the full equation (3.4*a*) within a vicinity of t_s, since the higher-order terms not shown in (3.4*b*) act locally as a contraction mapping. Further, our assumption that $\delta t = 0$ is the first time that a singularity forms, means that solutions to (3.4*b*) must not exist for $\delta t < 0$; hence at the first occurrence of separation, at least one of n_{11}, n_{22}, or n_{33} must necessarily be zero, and we will reorder (k_1, k_2, k_3) such that n_{11} vanishes. In addition, the coefficients n_{22}, n_{33}, z_1 cannot all be non-zero, since by solving for $\delta\lambda$, k_2, and k_3, it again follows that singularities exists for $\delta t < 0$. Without loss of generality, we assume that z_1 is zero, since if either n_{22} or n_{33} vanishes, the (k_1, k_2, k_3) coordinate system can be rotated further to eliminate z_1.

It follows that in some suitably oriented Lagrangian coordinate system the conditions $n_{11} = z_1 = 0$ are necessary at the time when separation starts. This implies two additional conditions on $x(\xi, t)$ and $z(\xi, t)$, besides the two conditions implicit in (3.1*a*). Since Lagrangian space–time is four-dimensional, in general we do not expect that more than four conditions can be satisfied at any time. Hence, in the remainder of this section we will assume that the values of the remaining derivatives can be completely arbitrary and in general non-zero.

However, when the functions x and z are not arbitrary, but restricted by constraints of symmetry in the flow, the latter assumption needs to be reconsidered, since the symmetry requires that various derivatives must vanish. Examples are two-dimensional flow, and the flows discussed in the next section.

Under the assumption that the remaining coefficients in the Taylor series have arbitrary values, the transformation

$$\tilde{z} = z - z(\xi_s, t), \quad \tilde{n} = n - n(\xi_s, t) - \lambda_s^{(2)} \tilde{z}^2, \tag{3.5a, b}$$

$$\tilde{k}_1 = k_1, \quad \tilde{k}_2 = \frac{n_{22} z_3 k_2 - n_{33} z_2 k_3}{(n_{22}^2 z_3^2 + n_{33}^2 z_2^2)^{\frac{1}{2}}}, \quad \tilde{k}_3 = \frac{n_{33} z_2 k_2 + n_{22} z_3 k_3}{(n_{22}^2 z_3^2 + n_{33}^2 z_2^2)^{\frac{1}{2}}}, \tag{3.5c–e}$$

where

$$\lambda_s^{(2)} = \frac{n_{22} n_{33}}{2(n_{22} z_3^2 + n_{33} z_2^2)}, \tag{3.5f}$$

eliminates the $\tilde{n}_{33}$ term. The final coordinate transform

$$l_1 = \tilde{k}_1 + \frac{\tilde{n}_{113}}{\tilde{n}_{111}} \tilde{k}_3, \quad l_2 = \tilde{k}_2, \quad l_3 = \tilde{k}_3, \tag{3.6a–c}$$

$$\bar{n} = \tilde{n} - \lambda_s^{(3)} \tilde{z}^3 - \mu_s \delta t \tilde{z}, \quad \bar{z} = \tilde{z}, \tag{3.6d, e}$$

where

$$\lambda_s^{(3)} = \frac{\tilde{n}_{111}^2 \tilde{n}_{333} - 3\tilde{n}_{111} \tilde{n}_{113} \tilde{n}_{133} + 2\tilde{n}_{113}^3}{6\tilde{n}_{111}^2 \tilde{z}_3^3}, \quad \mu_s = \frac{\tilde{n}_{111} \dot{\tilde{n}}_3 - \tilde{n}_{113} \dot{\tilde{n}}_1}{\tilde{n}_{111} \tilde{z}_3}, \tag{3.6f, g}$$

eliminates the $\bar{n}_{113}$, $\bar{n}_{333}$, and $\dot{\bar{n}}_3$ derivatives

The transformed position coordinate $\bar{n}$ corresponds to an oblique coordinate measured from a moving, curved line through the separation particle, viz.

$$\bar{n} = \bar{x} - \bar{x}_0(\bar{z}, t), \tag{3.7a}$$

where

$$\bar{x} = x - x(\xi_s, t), \quad \bar{z} = z - z(\xi_s, t), \tag{3.7b, c}$$

$$\bar{x}_0(\bar{z}, t) = \lambda_s \bar{z} + \lambda_s^{(2)} \bar{z}^2 + \lambda_s^{(3)} \bar{z}^3 + \mu_s \delta t \bar{z}. \tag{3.7d}$$

Note that the curved line $\bar{x} = \bar{x}_0(\bar{z}, t)$, which can be viewed as the line along which the separation initially develops (see below), does not have a singular shape at the first occurrence of separation.

The Taylor series expansions for $\bar{n}$ and $\bar{z}$ near the separation point become

$$\bar{n} = \tfrac{1}{2}\bar{n}_{22} l_2^2 + \sum_{ijk} \tfrac{1}{6}\bar{n}_{ijk} l_i l_j l_k + \ldots + \delta t \sum_i \dot{\bar{n}}_i l_i + \ldots \quad (\bar{n}_{113} = \bar{n}_{333} = \dot{\bar{n}}_3 = 0), \tag{3.8a}$$

$$\bar{z} = \bar{z}_2 l_2 + \bar{z}_3 l_3 + \ldots. \tag{3.8b}$$

The characteristics of the Jacobian equation (2.2) for y are, in terms of the new coordinates,

$$\frac{\mathrm{d}l_1}{\mathrm{d}y} = \frac{\rho H}{\rho_0 H_0} \{ -\bar{z}_3 \bar{n}_{22} l_2 + \ldots \}, \tag{3.9a}$$

$$\frac{\mathrm{d}l_2}{\mathrm{d}y} = \frac{\rho H}{\rho_0 H_0} \{ \bar{z}_3 (\tfrac{1}{2}\bar{n}_{111} l_1^2 + \tfrac{1}{2}\bar{n}_{133} l_3^2 + \dot{\bar{n}}_1 \delta t) + \ldots \}, \tag{3.9b}$$

$$\frac{\mathrm{d}l_3}{\mathrm{d}y} = \frac{\rho H}{\rho_0 H_0} \{ -\bar{z}_2 (\tfrac{1}{2}\bar{n}_{111} l_1^2 + \tfrac{1}{2}\bar{n}_{133} l_3^2 + \dot{\bar{n}}_1 \delta t) + \ldots \}, \tag{3.9c}$$

with a singularity occurring when all three right-hand-side expressions vanish (note that not all three are independent). Near the point s, (3.9*a*) is zero on a surface approximating the $l_2 = 0$ plane, while both (3.9*b*) and (3.9*c*) vanish at points depending on the nature of the quadratic expression $(\frac{1}{2}\bar{n}_{111} l_1^2 + \frac{1}{2}\bar{n}_{133} l_3^2)$. If this quadratic is hyperbolic, singular particles occur along hyperbolic lines regardless of the sign of δt. Thus, if $\delta t = 0$ is to be the first time that separation occurs, the quadratic must be elliptic, and of the same sign as the constant term when $\delta t < 0$. This requires $\bar{n}_{111}\bar{n}_{133} > 0$ and $\bar{n}_{111}\dot{\bar{n}}_1 < 0$; we will choose the positive l_1 direction such that

$$\bar{n}_{22}\bar{n}_{111} > 0, \quad \bar{n}_{22}\bar{n}_{133} > 0, \quad \bar{n}_{22}\dot{\bar{n}}_1 < 0. \tag{3.10a–c}$$

The Lagrangian description of the separation process can now be completed by the determination of y at times shortly before the initial occurrence of separation. At $t = t_s$ the boundary-layer approximation is obviously no longer valid because from the integral (2.6) it follows that y becomes infinite at the stationary point. However, the rate of growth near this point can be found by means of an asymptotic expansion. To find local scalings, we follow the guiding principles of Van Dyke (1975). In general, we attempt to scale the Lagrangian coordinates l_i and the position coordinates $\bar{n}$, $\bar{z}$ and y to variables L_i, N, Z, and Y such that in the inner region the Jacobian equation for Y, i.e.

$$J_L(N, Y, Z) = \begin{vmatrix} N_{L_1} & N_{L_2} & N_{L_3} \\ Y_{L_1} & Y_{L_2} & Y_{L_3} \\ Z_{L_1} & Z_{L_2} & Z_{L_3} \end{vmatrix} = \frac{\rho_0 H_0}{\rho H}, \tag{3.11}$$

has non-singular leading-order coefficients. This suggests that the δt term in (3.9*b*), which ensures the absence of singular points for $\delta t < 0$, should be retained. Further, for $\delta t = 0$ we want to match the solution close to the stationary particle to a solution for y which is regular away from this point. Thus we want to retain those terms that ensure the absence of singular points away from particle ξ_s at time $\delta t = 0$, i.e. the l_1^2 and l_3^2 terms in (3.9*b*) and the l_3 term in (3.9*a*). The appropriate scaling is therefore

$$l_1 = |\delta t|^{\frac{1}{2}} L_1, \quad l_2 = |\delta t|^{\frac{3}{4}} L_2, \quad l_3 = |\delta t|^{\frac{1}{2}} L_3, \tag{3.12a–c}$$

$$\bar{n} = |\delta t|^{\frac{3}{2}} N, \quad \bar{z} = |\delta t|^{\frac{1}{2}} Z, \quad y = |\delta t|^{-\frac{1}{4}} Y. \tag{3.12d–f}$$

These scalings suggest that the separation process occurs in a relatively thin strip, $\bar{n} \sim |\delta t|^{\frac{3}{2}}$ along a segment of the separation line $\bar{x} = \bar{x}_0(\bar{z}, t)$ of length $\bar{z} \sim |\delta t|^{\frac{1}{2}}$.

For the scaling (3.12), the solution for Y is most easily found by integration of (3.11) as in (3.9*a*), where L_2 and L_3 are eliminated in favour of N and Z, which are constant along the lines of integration, using (3.8). The result is

$$Y \sim \frac{\rho_{0s} H_{0s}}{\rho_s H_s} \left(\int_{-\infty}^{L_0} \frac{\mathrm{d}L}{(P(L; N, Z))^{\frac{1}{2}}} \pm \int_{L_1}^{L_0} \frac{\mathrm{d}L}{(P(L; N, Z))^{\frac{1}{2}}} \right), \tag{3.13a}$$

where

$$P(L; N, Z) = -\tfrac{1}{3}\bar{n}_{22}\{\bar{z}_3^2 \bar{n}_{111} L^3 + (3\bar{n}_{133} Z^2 - 6\dot{\bar{n}}_1 \bar{z}_3^2) L - 6\bar{z}_3^2 N\}, \tag{3.13b}$$

and $L_0(N, Z)$ is the real root of the cubic P. This root is a unique and continuous function of N and Z since P is a monotically decreasing function of L from (3.10).

The choice of sign of the square root in (3.13*a*), and the limits of integration are determined by the topology of the lines of constant N and Z. In physical space these

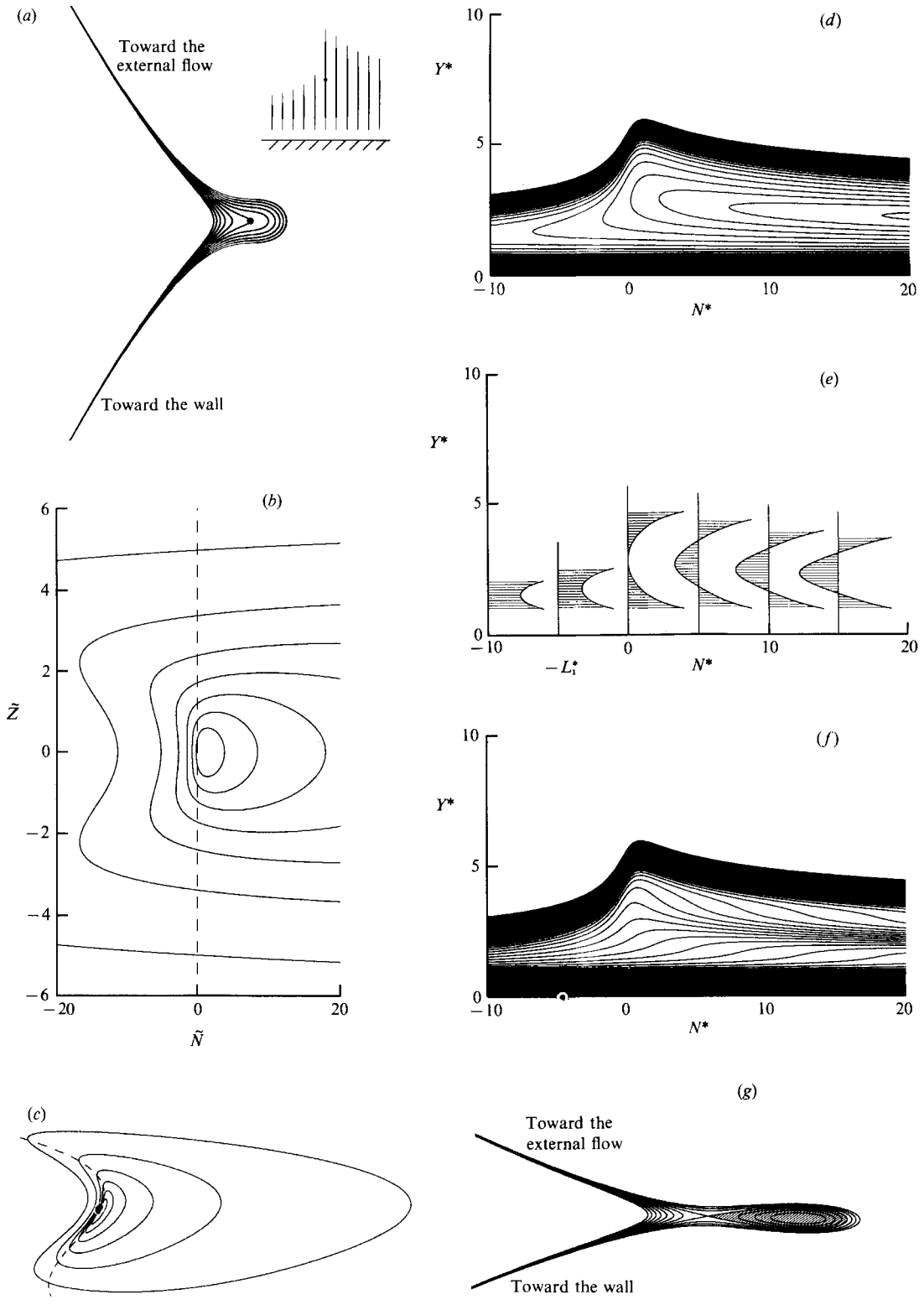

FIGURE 2(*a–g*). For caption see facing page.

lines are straight and pass vertically through the boundary layer, but in Lagrangian space they develop high curvature near point s on account of (3.8) and the scalings (3.12a, b, c). For, although the surface of constant z through the point s is asymptotically planar near s in Lagrangian space, the lines of constant x in this plane fold around and appear qualitatively as shown in figure 2(a). In this figure, the separation particle is indicated by a dot, and the inset at the upper right shows the same lines of constant x in the Eulerian plane of constant z. At the separation time, the fold at point s collapses to a cusp. The plane of constant z shown in figure 2(a) corresponds asymptotically to the $l_3 = 0$ plane, with the l_1 coordinate horizontally and the l_2 coordinate vertically. (The same structure occurs in planes $l_3 =$ constant $\neq 0$; in terms of the generalized coordinates defined in (3.14), figure 2(a) represents lines of constant N^* in the (L_1^*, L_2^*)-plane.)

The lines of constant N and Z can be divided into three segments corresponding to three asymptotic regions. This subdivision is schematically indicated by the variation in line thickness in figure 2(a). The lower segments start at the wall and extend upward towards the vicinity of the separation particle. Because the Jacobian is nowhere singular along these segments, the y-positions of the fluid particles remain finite on the boundary-layer scale, i.e. the scaled coordinate Y is small. Hence, these lower segments give rise to a layer of particles at the wall with a thickness comparable with that of the original boundary layer; this is shown schematically in figure 1.

Along the central segments, the lines of the constant N and Z pass through the vicinity of the separation particle. Here the y-position of the particles grows rapidly, and is given in scaled form by (3.13). Thus the central segments give rise to the intermediate, thicker, layer of particles shown in figure 1. The topology of the central segments in the Lagrangian domain, figure 2(a), determines the choice of sign in (3.13a). From (3.8) and (3.9) it follows that on integrating upwards, L_1 increases from large negative values towards $L_0(N, Z)$. Since Y increases, along this part the negative sign in (3.13a) applies. At position L_0, the lines of constant N and Z turn around in the Lagrangian domain and L_1 again tends to $-\infty$; along this second part the positive sign in (3.13a) applies.

Along the third segments, the lines of constant N and Z proceed upwards toward the external flow. As in the lower segments, the Jacobian is no longer small here. Thus the changes in y are finite on boundary-layer scale, and the third segments give rise to a layer of particles with a boundary-layer scale thickness, atop the central region, as shown in figure 1.

Hence, the separation structure is one in which the boundary layer divides into a central layer of physical thickness proportional to $Re^{-\frac{1}{2}}|\delta t|^{-\frac{1}{4}}$ between two 'sandwich' layers of thickness proportional to $Re^{-\frac{1}{2}}$.

The structure (3.13) is identical to the one obtained by Van Dommelen & Shen (1982) for two-dimensional separation, except that the coefficients now depend on the position Z along the describing line $\bar{x}_0$. A convenient way to illustrate the

FIGURE 2. Structure of asymmetric three-dimensional separation: (a) Lagrangian topology of vertical lines through the boundary layer near the separation particle; (b) contours of the scaled boundary-layer thickness $\tilde{Y}^+ = 5\frac{1}{2}, 5, 4\frac{1}{2}, \ldots, 2\frac{1}{2}$ in scaled, oblique coordinates; (c) possible actual appearance of contours of boundary-layer thickness (schematic); (d) contours of the scaled velocity $L_1^* = 0, \pm 1, \pm 2 \ldots$ in scaled coordinates; (e) $-L_1^*$ velocity profiles; (f) contours of the scaled vorticity $\partial L_1^*/\partial Y^* = 0, \pm 1, \pm 2, \ldots$; ($g$) topology of vertical lines through the boundary layer for times beyond the first singularity.

influence of the position Z is to scale out the coefficients using a procedure similar to Van Dommelen (1981):

$$L_1 = \beta_2 \tilde{L}_1 = \beta_2(\tilde{Z}^2+1)^{\frac{1}{2}} L_1^*, \quad L_2 = \beta_0 \beta_2^{\frac{3}{2}} \tilde{L}_2 = \beta_0 \beta_2^{\frac{3}{2}}(\tilde{Z}^2+1)^{\frac{3}{4}} L_2^*, \quad (3.14a, b)$$

$$N = \alpha\beta_2^3 \tilde{N} = \alpha\beta_2^3(\tilde{Z}^2+1)^{\frac{3}{2}} N^*, \quad Y = \frac{\tilde{Y}}{\gamma\beta_2^{\frac{1}{2}}} = \frac{Y^*}{\gamma\beta_2^{\frac{1}{2}}(\tilde{Z}^2+1)^{\frac{1}{4}}}, \quad Z = \frac{\beta_2}{\beta_1}\tilde{Z}, \quad (3.14c\text{–}e)$$

where the variables with a tilde scale out the Taylor series coefficients, the variables with asterisks scale out Z, and

$$\alpha = \tfrac{1}{3}\overline{n}_{111}, \quad \gamma = (\tfrac{1}{3}\overline{z}_3^2\,\overline{n}_{22}\,\overline{n}_{111})^{\frac{1}{2}} \frac{\rho_s H_s}{\rho_{0s} H_{0s}}, \quad (3.14f, g)$$

$$\beta_0 = \frac{\overline{z}_3\,\overline{n}_{111}}{(\overline{z}_3^2\,\overline{n}_{22}\,\overline{n}_{111})^{\frac{1}{2}}}, \quad \beta_1 = \left(\frac{\overline{n}_{133}}{\overline{z}_3^2\,\overline{n}_{111}}\right)^{\frac{1}{2}}, \quad \beta_2 = \left(-\frac{2\dot{\overline{n}}_1}{\overline{n}_{111}}\right)^{\frac{1}{2}}. \quad (3.14h\text{–}j)$$

In terms of the variables with asterisks (3.13) reduces to

$$Y^* \sim \int_{-\infty}^{L_0^*} \frac{\mathrm{d}L^*}{(2N^*-3L^*-L^{*3})^{\frac{1}{2}}} \pm \int_{L_1^*}^{L_0^*} \frac{\mathrm{d}L^*}{(2N^*-3L^*-L^{*3})^{\frac{1}{2}}}, \quad (3.14k)$$

where
$$L_0^*(N^*) = I(N^*), \quad (3.15a)$$

and the function I is the inverse to the cubic $N^* = \frac{1}{2}I^3 + \frac{3}{2}I$, i.e.

$$I(N^*) = (N^* + (1+N^{*2})^{\frac{1}{2}})^{\frac{1}{3}} + (N^* - (1+N^{*2})^{\frac{1}{2}})^{\frac{1}{3}}. \quad (3.15b)$$

The values of β_1/β_2, $\alpha\beta_2^3$, and $\gamma\beta_2^{\frac{1}{2}}$ depend on the choice of the Eulerian coordinates (x, z), but not on the definition of the Lagrangian coordinates.

An alternative expression for Y^* can be found in terms of the incomplete elliptic integral of the first kind $F(\phi \mid m)$:

$$Y^*(L_1^*, N^*) \sim \frac{2}{\Lambda} F\left(\frac{\pi}{2}\middle| m\right) \pm \frac{1}{\Lambda} F(\phi \mid m), \quad (3.16a)$$

where
$$\Lambda(N^*) = (3(L_0^{*2}+1))^{\frac{1}{4}}, \quad m(N^*) = \frac{1}{2} + \frac{3L_0^*}{4\Lambda^2}, \quad (3.16b, c)$$

$$\phi(L_1^*, N^*) = 2\arctan\left(\frac{(L_0^*-L_1^*)^{\frac{1}{2}}}{\Lambda}\right). \quad (3.16d)$$

Elliptic integrals are distorted identity functions, (in particular $F(\phi \mid 0) = \phi$ exactly), so that the arctan is responsible for the major variations in Y along the characteristics.

Further terms in the asymptotic expansions (3.8) and (3.16) can be found in principle. We note that the next term in the expression for Y does not involve a logarithmic correction, even though logarithmic second-order terms do arise for the symmetric flows studied in the next section.

We now turn to the physical interpretation of these results. The boundary-layer thickness is asymptotically determined by the position of the upper particle layer in figure 1; letting $L_1^* \to -\infty$ along the positive branch of (3.16a), we obtain the scaled boundary-layer thickness as

$$Y^{+*}(N^*) \sim \frac{4}{\Lambda} F\left(\frac{\pi}{2}\middle| m\right). \quad (3.17)$$

The function $Y^{+*}(N^*)$ gives the general shape of the boundary-layer thickness in a cross-section of constant z. For large values of N^* the boundary-layer thickness decays toward zero much more slowly than suggested by the sketch in figure 1. Nevertheless, at the outer edges of the thin separation region, the solution still matches with that at finite values of y; for from (3.12), (3.14), and (3.16)

$$y^+ \sim \frac{4\alpha^{\frac{1}{6}}}{3^{\frac{1}{4}}2^{\frac{1}{6}}\gamma} F\left(\frac{\pi}{2}\middle|\frac{1}{2}\pm\frac{\sqrt{3}}{4}\right)\frac{1}{|\bar{n}|^{\frac{1}{6}}} \quad \text{for} \quad |\delta t|^{\frac{3}{2}} \ll |\bar{n}| \ll 1. \tag{3.18}$$

To show the dependence of the boundary-layer thickness on the coordinate z, contours of constant $\tilde{Y}^+$ in the $(\tilde{N}, \tilde{Z})$-plane are plotted in figure 2(*b*). Note that the coordinate $\tilde{N}$ is measured from the oblique, curved, separation line. Actual lines of constant boundary-layer thickness might, for example, appear as sketched in figure 2(*c*), which has been drawn by taking $|\delta t| = 0.06$ and unit values for various coefficients in (3.7) and (3.14). Asymptotically, the boundary-layer thickness has the form of a crescent-shaped ridge. The crescent shape is long and thin, i.e. quasi-two-dimensional, because from (3.12) the $\bar{n}$ lengthscale is asymptotically shorter than the $\bar{z}$ lengthscale (note that for three-dimensional *steady* separation Smith 1978 has proposed a quasi-two-dimensional structure). In an Eulerian numerical calculation, the development of such a crescent-shaped ridge may be a possible diagnostic indicating the presence of a singularity.

Evidence of this type of singularity is provided by Ragab's (1986) calculations for impulsively started flow past a 4:1 prolate spheroid inclined at a 30° angle of attack. His results strongly suggest that the displacement thickness becomes unbounded away from the symmetry line. However, it is not possible to deduce the shape of the singularity from the results presented.

A point of interest is the decay of the boundary-layer thickness along the describing line for large $\tilde{Z}$. From (3.12), (3.14), and (3.16),

$$y^+ \sim \frac{1}{\gamma\beta_1^{\frac{1}{2}}} Y^{+*}\left(\frac{\bar{n}}{\alpha\beta_1^3|\bar{z}|^3}\right)\frac{1}{|\bar{z}|^{\frac{1}{2}}} \quad \text{for} \quad |\delta t|^{\frac{1}{2}} \ll |\bar{z}| \ll 1. \tag{3.19}$$

Hence for increasing $\bar{z}$, the separation structure expands in the $\bar{n}$-direction, while the thickness of the boundary-layer decreases.

The particle propagation velocity $\dot{\bar{n}}$ which gives rise to the accumulation of particles at the separation line is, according to (3.8*a*), given to leading order by

$$\dot{\bar{n}} \sim |\delta t|^{\frac{1}{2}}\dot{\bar{n}}_1 L_1. \tag{3.20}$$

To describe this in the more familiar Eulerian coordinates, the transcendental relationship (3.16) must be inverted to the form

$$L_1^* = L_1^*(N^*, Y^*). \tag{3.21}$$

The inversion has been performed numerically, and in figure 2(*d*) we present contours of L_1^* in the (N^*, Y^*)-plane. From (3.14),

$$\dot{\bar{n}} \sim -|\delta t|^{\frac{1}{2}}\tfrac{3}{2}\alpha\beta_2^3(\tilde{Z}^2+1)^{\frac{1}{2}} L_1^*\left(\frac{\tilde{N}}{(\tilde{Z}^2+1)^{\frac{3}{2}}}, \tilde{Y}(\tilde{Z}^2+1)^{\frac{1}{4}}\right). \tag{3.22}$$

It follows that the lines of constant L_1^* shown in figure 2(*d*) describe the shapes of the lines of constant $\dot{\bar{n}}$ in cross-sections of constant $\bar{z}$ through the separation structure.

They also give the asymptotic shape of the lines of constant velocity components $\dot{x}$ and $\dot{z}$ and density ρ in these cross-sections, since

$$(\dot{x},\dot{z},\rho) = (\dot{x}_s,\dot{z}_s,\rho_s) + |\delta t|^{\frac{1}{2}}\left((\dot{\bar{x}}_1,\dot{\bar{z}}_1,\bar{\rho}_1)\,\beta_2(\tilde{Z}^2+1)^{\frac{1}{2}}L_1^* + (\dot{\bar{x}}_3,\dot{\bar{z}}_3,\bar{\rho}_3)\frac{\beta_2}{\beta_1\bar{z}_3}\tilde{Z}\right) + \ldots. \tag{3.23}$$

We note that the topology of figure 2(*d*) for $|\delta t| \approx 0$ seems quite close to the computed lines of constant velocity presented by Van Dommelen (1981) for finite $|\delta t|$, and thus lines of constant velocity might be a useful indication of an incipient unsteady separation.

The next point of interest is the shape of the velocity profiles. According to (3.23), in Eulerian space the velocity profiles must develop a large flat region of nearly constant velocity as separation is approached. However, if we accept the numerical results of Van Dommelen (1981), this flat region is only evident extremely close to the singularity, so that resolution problems or finite-Reynolds-number effects tend to obscure the phemomenon. From (3.23) and figure 2(*d*), the velocity profiles near an incipient three-dimensional separation must have a local maximum or minimum in velocity. However, this is not necessarily a precise indication of incipient separation. For example, in the case of the circular cylinder, a minimum in the velocity profiles develops relatively quickly, after $\frac{1}{6}$ diameter motion, yet separation occurs much later, after $\frac{3}{4}$ diameter motion. Figure 2(*e*) shows the shape of the velocity profiles near the interior extrema. The shapes of the velocity profiles in the sandwich layers at the edges of figure 2(*e*) cannot be found from asymptotic analysis since they depend on the precise details of the earlier evolution (cf. the remarks below (3.24) and Part 2).

A more significant sign of the start of separation might be a transverse expansion of the lines of constant vorticity near the velocity minimum/maximum; since the above analysis is inviscid to leading order, the vorticity lines closely follow the motion of the boundary-layer particles. In the boundary-layer approximation, the vorticity is the y-derivative of the velocity distribution. The corresponding asymptotic topology of contours of $\partial L_1^*/\partial Y^*$ is shown in figure 2(*f*). This topology seems close to the computed vorticity lines presented by Van Dommelen (1981) for a time near separation.

The asymptotic structures of the upper and lower vorticity layers are similar to the two-dimensional case (Van Dommelen 1981). Expressed in terms of Eulerian coordinates, they take the form of regular Taylor expansions:

$$(\dot{x},\dot{y},\dot{z},\dot{\rho}) = \sum_{mnr\geqslant 0} \bar{x}^m\bar{z}^n\delta t^r(u^-_{mnr}(y), v^-_{mnr}(y), w^-_{mnr}(y), \rho^-_{mnr}(y)), \tag{3.24a}$$

and

$$(\dot{x},\dot{\tilde{y}},\dot{z},\dot{\rho}) = \sum_{mnr\geqslant 0} \bar{x}^m\bar{z}^n\delta t^r(u^+_{mnr}(\tilde{y}), v^+_{mnr}(\tilde{y}), w^+_{mnr}(\tilde{y}), \rho^+_{mnr}(\tilde{y})), \tag{3.24b}$$

respectively, where the sums run over the non-negative integers, and the Prandtl transformation, $\tilde{y} = y - y^+(\bar{x},\bar{z},\delta t)$, describes the motion of the upper layer.

Substituting (3.24) into the boundary-layer equations, we find that the $u^\pm_{mnr}, w^\pm_{mnr}, \rho^\pm_{mnr}$, $(m,n\geqslant 0, r\geqslant 1)$ and the $v^\pm_{mnr}$, $(m,n,r\geqslant 0)$ are determined in terms of the $(u^\pm_{mn0}, w^\pm_{mn0}, \rho^\pm_{mn0})$, but that these latter functions are indeterminate owing to the dependence of the solution on earlier times. The $(u^\pm_{mn0}, w^\pm_{mn0}, \rho^\pm_{mn0})$ must, however, satisfy the boundary conditions (2.5*a*) at the wall, and match both at the outer edge of the boundary layer (see (2.5*b*)), and with the central inviscid low-vorticity region.

At fixed N and Z, the latter matching conditions yield, from inverting (3.16) and using (3.23),

$$(u^-_{000}, w^-_{000}, \rho^-_{000}) \sim (\dot{x}_s, \dot{z}_s, \rho_s) - (\dot{\bar{x}}_1, \dot{\bar{z}}_1, \bar{\rho}_1)\frac{4}{\gamma^2}\frac{1}{y^2} \quad \text{as} \quad y \to +\infty, \tag{3.25a}$$

$$(u^+_{000}, w^+_{000}, \rho^+_{000}) \sim (\dot{x}_s, \dot{z}_s, \rho_s) - (\dot{\bar{x}}_1, \dot{\bar{z}}_1, \bar{\rho}_1)\frac{4}{\gamma^2}\frac{1}{\tilde{y}^2} \quad \text{as} \quad \tilde{y} \to -\infty. \tag{3.25b}$$

Asymptotic matching conditions can also be derived as $|N|, |Z| \to \infty$, as Van Dommelen (1981) has done for two-dimensional flows.

A final point of interest is the 'accessibility' of the region of flow beyond the time of initial separation. In a steady Eulerian computation, Cebeci, Khattab & Stewartson (1981) took the accessible region to be the domain where a boundary-layer solution can be found (whether it is still an asymptotically correct solution of the Navier–Stokes equations in the presence of interaction or not). In the Lagrangian case, some care is needed, because the singular continuity equation is integrated separately. Numerical experiments such as the one in Part 2 do in fact suggest that the non-singular momentum equations can be integrated past the separation singularity without apparent difficulty. When that is done, the vertical lines through the boundary layer appear in Lagrangian space as shown in figure 2(*g*) rather than figure 2(*a*). For the shaded particles, y is indeterminate; these particles may be thought of as having disappeared at infinite y. Yet the continuity equation can still be integrated along all lines of constant $\bar{n}$ and $\bar{z}$ which start at the wall. A singularity develops only on the line passing through the saddle point in figure 2(*g*), which for $0 < \delta t \ll 1$ corresponds to a singular line segment

$$\tilde{N} \sim +(1-\tilde{Z}^2)^{\frac{3}{4}}. \tag{3.26}$$

However, the solution so obtained must be considered meaningless at least for all particles which have at some previous time passed through the singular curve. For that reason, we define the region of inaccessibility as those stations (x, z) that contain particles that have at any time been on the singular curve. Initially, the region of inaccessibility will primarily expand in the z-direction through the scaling (3.12*e*). In the n-direction it will expand by means of the motion of the describing line (3.7) and additionally through the motion of the particles which propagate downstream away from the singular curve. Thus, the region of inaccessibility extends over a finite surface area, rather than just the curve (3.26), in agreement with the steady Eulerian definition of Cebeci *et al.* (1981).

Naturally, the singularity structure derived here will not remain asymptotically correct arbitrarily close to $t = t_s$, because the normal velocity above the central inviscid region becomes infinite at $t = t_s$. From a study of the Navier–Stokes equations it is found that the singularity is smoothed out when a 'triple-deck' interaction comes into operation for $\delta t = O(Re^{-\frac{2}{11}})$, at which point the scaled boundary-layer thickness is $O(Re^{\frac{1}{22}})$. Because the singularity is quasi-two-dimensional, the scalings and governing equations are essentially those derived by Elliott *et al.* (1983) for two-dimensional flows, but with the addition of a passive z-momentum equation. In the central interaction problem, the coordinate z, which has an interaction lengthscale $O(Re^{-\frac{1}{11}})$, only appears as a parameter. However, it is not clear whether the singularity will be completely removed by the interaction (Smith 1987).

4. Three-dimensional symmetric separation

In the previous section a separation singularity structure was derived assuming that the flow was arbitrary, an assumption that might be appropriate for flow past an asymmetric body. However, in the case of a spheroid at relatively small angles of attack it is likely that separation first occurs on one of the symmetry lines; indeed numerical calculations confined to the symmetry line have been performed on this basis (Wang & Fan 1982; Cebeci *et al.* 1984). In §4.1 below we derive the form of the singularity appropriate for separating flows where the separation line crosses a symmetry line normally.

However, this is not the only type of symmetric separation of interest. When a sphere is impulsively rotated about a diameter, centripetal effects generate a boundary-layer flow towards the equator. After a finite time an equatorial singularity develops as a result of a boundary-layer collision. The structure of this singularity on the symmetry line has been determined by Banks & Zaturska (1979), and Simpson & Stewartson (1982*a*). In this case the separation line coincides with the symmetry line. Similar singularities occur after a finite time at the apex of a horizontal circular cylinder which is impulsively heated (Simpson & Stewartson 1982*b*), at the inner bend of a uniformly curved pipe through which flow is impulsively started (Lam 1988), and at the stagnation points on a two-dimensional cylinder in oscillating flow as a result of steady streaming effects (Vasantha & Riley 1988).

A more general form of the singularity generated by two symmetric colliding boundary layers on a smooth wall would first develop at a point rather than along the entire symmetry line. For example, such a singularity might develop on the equator of an ellipsoid which is rotated about one of its principal axes, or in starting flow through a curved pipe with non-uniform curvature, or at the apex of a heated ellipsoid. In §4.2 the three-dimensional structure of such a singularity is derived. The results on the symmetry line agree with those of previous authors, but the simplicity of the Lagrangian approach allows us to determine additionally the singularity structure off this line. The latter is a necessary preliminary in order to formulate subsequent asymptotic stages in the separation process.

Another class of separation singularities is rotationally symmetric about the separation point, so that the separation line degenerates to a point. For example, singularities develop after a finite time on the axis of a spinning disc or sphere whose direction of rotation is impulsively reversed (Bodonyi & Stewartson 1977; Banks & Zaturska 1981; Stewartson, Simpson & Bodonyi 1982; Van Dommelen 1987), and at the apex of a sphere which is impusively heated (Brown & Simpson 1982; Awang & Riley 1983). The structures of these singularities, which differ owing to the presence and absence of swirl, are derived in §§4.3 and 4.4 respectively. The results on the axis agree with those of previous authors, while the singularity structures off the axis are new.

4.1. *Lateral symmetry*

When the boundary-layer flow is symmetrical about a line along the surface of the body, the describing line of separation must either cross the symmetry line normally or coincide with it. In this subsection we will address the case of normal crossing, leaving the second possibility to the next subsection. The case studied here applies to flows such as separation at the symmetry plane of spheroids at relatively small angles of attack (Wang & Fan 1982; Cebeci *et al.* 1984). More generally, it may occur in flows in which the fluid in a symmetry plane loses kinetic energy, e.g. through an

adverse pressure gradient, leading to flow reversal. It includes the degenerate but important case of two-dimensional separation.

For consistency with §3, we identify the compressed coordinate n with x, where x is the coordinate along the symmetry plane. Hence in Lagrangian space, the (ξ, η)-plane is the symmetry plane, so that x is an even function of ζ and z an odd function. With this assumption the analysis is a simpler version of the one in the previous section. The only transformation of the Lagrangian coordinate system needed is a rotation around the ζ-axis to eliminate the x_{12} derivative. Also, the discussion concerning which derivatives must be zero if t_s is the first separation time (see (3.4) and following) can be restricted to the symmetry plane to show that the second-order derivative which is forced to be zero must lie within the symmetry plane.

Hence the structure of the separation process remains basically unchanged, although the describing line of separation simplifies, and is now symmetric about the symmetry line $z = 0$ (cf. (3.7)):

$$\bar{n} = x - x(\xi_s, t) - \frac{x_{33}}{2z_3^2} z^2. \tag{4.1}$$

A degenerate case is two-dimensional flow, where x is totally independent of ζ, and the separation line becomes a straight generator in the z-direction. In addition, the coefficient β_1 vanishes, which suppresses the decay of the boundary-layer thickness with z. The resulting structure is described in detail by Van Dommelen (1981).

Thus lateral symmetry, or more strongly two-dimensionality, does not fundamentally alter the separation process. This conclusion is consistent with the symmetry line calculations of Cebeci *et al.* (1984). Since the velocity profiles have a local minimum near the separation particle (figure 2*e*), flow reversal will usually have to occur before the flow can separate.

4.2. *Symmetric boundary-layer collision*

When the describing line coincides with the symmetry line, significant changes in structure are unavoidable, since the flow is symmetric while the separation structure illustrated in figure 2 is asymmetrical. Yet this case is physically important, since it occurs on the equator of a sphere given a spinning motion (cf. Part 2; Banks & Zaturska 1979), at the apex of a horizontal, heated circular cylinder (Simpson & Stewartson 1982*b*), at the inner bend in flow through a uniformly curved pipe (Lam 1988), and at the stagnation points on a circular cylinder in oscillating flow (Vasantha & Riley 1988). It can also be expected in other flows in which the fluid is driven towards a plane of symmetry. For example, if an ellipsoid rather than a sphere or spheroid is given a spinning motion about one of its principle axes, the separation may initially occur at a single point rather than in the entire symmetry plane simultaneously. This may also be the case for more general heated bodies than a circular cylinder with a vertical symmetry plane, such as ellipsoids.

We identify the compressed coordinate n again with x, but now we take x to be the coordinate normal to the symmetry plane. In Lagrangian space, the (η, ζ)-plane is now the symmetry plane, so that x is an odd function of ξ while z is an even function. A singularity occurs when $x_{,\xi}$ first vanishes at the symmetry plane, since the derivatives $x_{,\eta}$ and $x_{,\zeta}$ are zero by symmetry. Since the first occurrence of a zero value must occur where $x_{,\xi}$ is a minimum, the second-order derivatives $x_{\xi\eta}$ and $x_{\xi\zeta}$ must vanish, while the other second-order derivatives are zero by symmetry.

The fact that all the second-order derivatives are zero invalidates the scalings for η and y made in the previous section (e.g. (3.12), (3.14)); hence a separate analysis

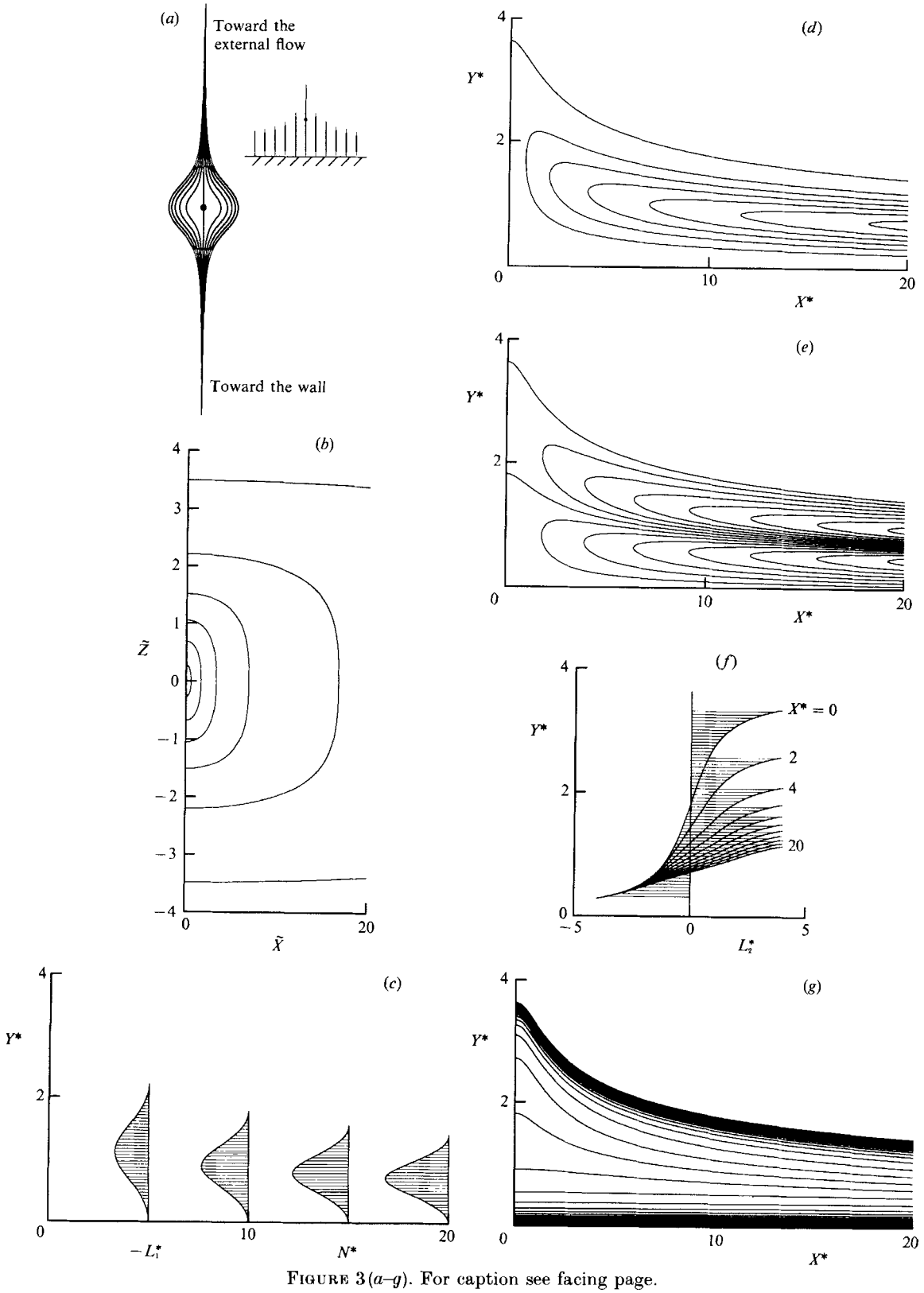

FIGURE 3(*a–g*). For caption see facing page.

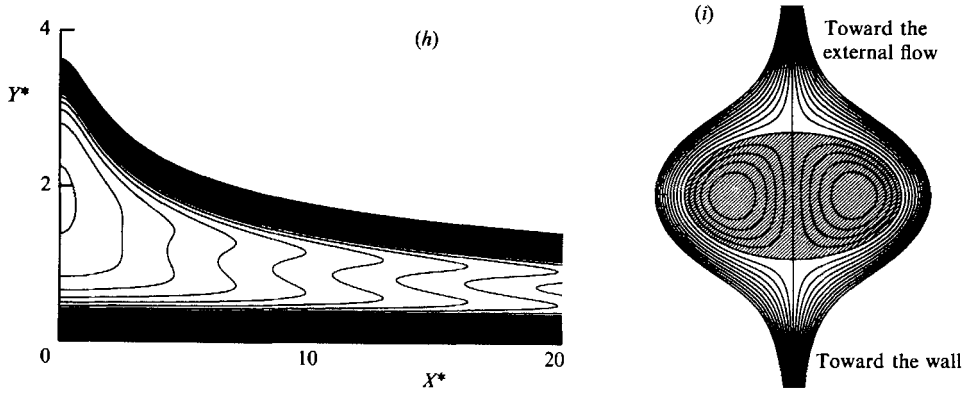

FIGURE 3. Structure of symmetric three-dimensional separation: (*a*) Lagrangian topology of physically vertical lines; (*b*) contours of boundary-layer thickness $\tilde{Y}^+ = 3\frac{1}{2}, 3, 2\frac{1}{2}, \ldots, 1$; (*c*) $-L_1^*$ velocity profiles; (*d*) contours of $L_1^* = 0, \frac{1}{2}, 1, 1\frac{1}{2}, \ldots$; (*e*) contours of $\partial L_1^*/\partial Y^* = 0, \pm 1, \pm 2, \ldots$; (*f*) L_2^* velocity profiles for flow parallel to the symmetry plane; (*g*) contours of $L_2^* = 0, \pm 1, \pm 2, \ldots$; (*h*) contours of $\partial L_2^*/\partial Y^* = 1, 2, 3, \ldots$; (*i*) Lagrangian topology of physically vertical lines beyond the first singularity.

with significant modifications is needed. Proceeding along similar lines as in the previous section, a local Lagrangian coordinate system k_1, k_2, k_3 is introduced with origin at the separation particle, but with the same orientation as the original axis system. A rotation of this coordinate system around the k_1 axis,

$$\tilde{k}_1 = \xi, \quad \tilde{k}_2 = \frac{z_3 k_2 - z_2 k_3}{(z_2^2+z_3^2)^{\frac{1}{2}}}, \quad \tilde{k}_3 = \frac{z_2 k_2 + z_3 k_3}{(z_2^2+z_3^2)^{\frac{1}{2}}}, \tag{4.2a–c}$$

$$\tilde{x} = x, \quad \tilde{z} = z - z(\xi_s, t), \tag{4.2d, e}$$

can be made to eliminate the $\tilde{z}_2$ derivative. The shearing transformation

$$l_1 = \xi, \quad l_2 = \tilde{k}_2 + \frac{\tilde{x}_{123}}{\tilde{x}_{122}}\tilde{k}_3, \quad l_3 = \tilde{k}_3, \tag{4.3a–c}$$

$$\bar{x} = x, \quad \bar{z} = z - z(\xi_s, t), \tag{4.3d, e}$$

eliminates the $\bar{x}_{123}$ derivative, resulting in the Taylor series expansions

$$x \sim \tfrac{1}{6}\bar{x}_{111} l_1^3 + \tfrac{1}{2}\bar{x}_{122} l_1 l_2^2 + \tfrac{1}{2}\bar{x}_{133} l_1 l_3^2 + \ldots + \delta t \dot{\bar{x}}_1 l_1 + \ldots, \tag{4.4a}$$

$$\bar{z} \sim \bar{z}_3 l_3 + \ldots. \tag{4.4b}$$

The expressions for the characteristics of the Jacobian equation for y become

$$\frac{\mathrm{d}l_1}{\mathrm{d}y} = \frac{\rho H}{\rho_0 H_0} l_1 \{-\bar{z}_3 \bar{x}_{122} l_2 + \ldots\}, \tag{4.5a}$$

$$\frac{\mathrm{d}l_2}{\mathrm{d}y} = \frac{\rho H}{\rho_0 H_0} \{\bar{z}_3 (\tfrac{1}{2}\bar{x}_{111} l_1^2 + \tfrac{1}{2}\bar{x}_{122} l_2^2 + \tfrac{1}{2}\bar{x}_{133} l_3^2 + \delta t \dot{\bar{x}}_1) + \ldots\}. \tag{4.5b}$$

In order to avoid singularities for $\delta t < 0$, the quadratic in (4.5*b*) must be elliptic and of opposite sign to $\dot{\bar{x}}_1$. Since $x_{,\xi}$ is initially positive, cf. (2.1), it follows from (4.4*a*) and (4.5*b*) that at a first zero

$$\bar{x}_{111} > 0, \quad \bar{x}_{122} > 0, \quad \bar{x}_{133} > 0, \quad \dot{\bar{x}}_1 < 0. \tag{4.6a–d}$$

The characteristics (4.5) are again the lines of constant x and z. The topology of the lines of constant x in the (l_1, l_2)-plane of constant z is shown in figure 3(*a*). The characteristic through point s remains straight by symmetry. This can be compared to the asymmetric case figure 2(*a*), where the separation characteristic develops a cusp at $\delta t = 0$. This difference in the characteristics results in a different separation structure.

Appropriate local scalings near separation can be found using arguments similar to those of the previous section:

$$l_1 = |\delta t|^{\frac{1}{2}}\beta_2 \tilde{L}_1 = |\delta t|^{\frac{1}{2}}\beta_2(\tilde{Z}^2+1)^{\frac{1}{2}}L_1^*, \tag{4.7a}$$

$$l_2 = |\delta t|^{\frac{1}{2}}\beta_0\beta_2 \tilde{L}_2 = |\delta t|^{\frac{1}{2}}\beta_0\beta_2(\tilde{Z}^2+1)^{\frac{1}{2}}L_2^*, \tag{4.7b}$$

$$x = |\delta t|^{\frac{3}{2}}\alpha\beta_2^3 \tilde{X} = |\delta t|^{\frac{3}{2}}\alpha\beta_2^3(\tilde{Z}^2+1)^{\frac{3}{2}}X^*, \tag{4.7c}$$

$$y = \frac{\tilde{Y}}{|\delta t|^{\frac{1}{2}}\gamma\beta_2} = \frac{Y^*}{|\delta t|^{\frac{1}{2}}\gamma\beta_2(\tilde{Z}^2+1)^{\frac{1}{2}}}, \quad \bar{z} = |\delta t|^{\frac{1}{2}}\frac{\beta_2}{\beta_1}\tilde{Z}, \tag{4.7d, e}$$

$$\alpha = \tfrac{1}{3}\bar{x}_{111}, \quad \gamma = (\tfrac{1}{3}\bar{z}_3^2\,\bar{x}_{122}\,\bar{x}_{111})^{\frac{1}{2}}\frac{\rho_s H_s}{\rho_{0s} H_{0s}}, \tag{4.7f, g}$$

$$\beta_0 = \frac{\bar{z}_3\,\bar{x}_{111}}{(\bar{z}_3^2\,\bar{x}_{122}\,\bar{x}_{111})^{\frac{1}{2}}}, \quad \beta_1 = \left(\frac{\bar{x}_{133}}{\bar{z}_3^2\,\bar{x}_{111}}\right)^{\frac{1}{2}}, \quad \beta_2 = \left(-\frac{2\dot{\bar{x}}_1}{\bar{x}_{111}}\right)^{\frac{1}{2}}. \tag{4.7h–j}$$

The continuity integral becomes

$$Y^* = \int_0^{L_0^*} \frac{\mathrm{d}L^*}{(L^*(2X^*-3L^*-L^{*3}))^{\frac{1}{2}}} \pm \int_{L_1^*}^{L_0^*} \frac{\mathrm{d}L^*}{(L^*(2X^*-3L^*-L^{*3}))^{\frac{1}{2}}}, \tag{4.8a}$$

where

$$L_0^*(X^*) = I(X^*). \tag{4.8b}$$

This can be written as an elliptic integral similar to (3.16),

$$Y^*(L_2^*, X^*) \sim \frac{2}{\Lambda}F\left(\frac{\pi}{2}\middle| m\right) \pm \frac{1}{\Lambda}F(\phi\,|\,m), \tag{4.9a}$$

where

$$\Lambda(X^*) = (3(L_0^{*2}+1)\,(L_0^{*2}+3))^{\frac{1}{4}}, \quad m(X^*) = \frac{1}{2} - \frac{3L_0^{*2}+6}{4\Lambda^2}, \tag{4.9b, c}$$

$$\phi(L_2^*, X^*) = 2\arctan\left(\frac{1}{\Lambda}\left[(L_0^{*2}+3)\left(\frac{L_0^*}{L_1^*}-1\right)\right]^{\frac{1}{2}}\right). \tag{4.9d}$$

Note that instead of using L_1^* as the independent variable, there is an advantage in using L_2^*, as given implicitly by the relation

$$L_1^*(L_2^*, X^*) = (L_2^{*2}+1)^{\frac{1}{2}} I(X^*/(L_2^{*2}+1)^{\frac{3}{2}}), \tag{4.9e}$$

since at the symmetry line the solution is regular in terms of L_2^*:

$$Y^*(L_2^*, 0) \sim \frac{2}{\sqrt{3}}(\tfrac{1}{2}\pi + \arctan L_2^*). \tag{4.10}$$

Contours of the boundary-layer thickness $\tilde{Y}^+$ in the $(\tilde{X}, \tilde{Z})$-plane are shown in figure 3(*b*). The asymptotic relations for large $|\tilde{X}|$ and $|\tilde{Z}|$, corresponding to (3.18) and (3.19), are

$$y^+ \sim \frac{4\alpha^{\frac{1}{3}}}{3^{\frac{1}{4}}2^{\frac{1}{3}}\gamma} F\left(\frac{\pi}{2}\middle|\frac{1}{2}-\frac{\sqrt{3}}{4}\right)\frac{1}{|x|^{\frac{1}{3}}} \quad \text{for} \quad |\delta t|^{\frac{3}{2}} \ll |x| \ll 1, \tag{4.11}$$

$$y^+ \sim \frac{1}{\gamma\beta_1} Y^{*+}\left(\frac{x}{\alpha\beta_1^3|\bar{z}|^3}\right)\frac{1}{|\bar{z}|} \quad \text{for} \quad |\delta t|^{\frac{1}{2}} \ll |\bar{z}| \ll 1. \tag{4.12}$$

The velocity components and density in the neighbourhood of the stationary point are given by

$$\dot{x} \sim -|\delta t|^{\frac{1}{2}}\tfrac{3}{2}\alpha\beta_2^3(\tilde{Z}^2+1)^{\frac{1}{2}}L_1^*, \tag{4.13a}$$

$$(\dot{z}, \rho) \sim (\dot{z}_s, \rho_s) + |\delta t|^{\frac{1}{2}}\left((\dot{\bar{z}}_2, \bar{\rho}_2)\beta_0\beta_2(\tilde{Z}^2+1)^{\frac{1}{2}}L_2^* + (\dot{\bar{z}}_3, \bar{\rho}_3)\frac{\beta_2}{\beta_1\bar{z}_3}\tilde{Z}\right). \tag{4.13b}$$

Hence L_1^* can be interpreted as the velocity component towards the symmetry plane. The scaled velocity profile, $-L_1^*$, is illustrated in figure 3(*c*) at a number of X^* stations. Note that the profiles of the velocity component away from the symmetry plane must have an internal minimum in order that this separation process can occur. Contours of L_1^*, and the corresponding vorticity component, $\partial L_1^*/\partial Y^*$, are illustrated in figures 3(*d*) and 3(*e*) respectively. In cross-sections of constant z, the variations in velocity parallel to the symmetry plane are proportional to L_2^*. L_2^* velocity profiles are given in figure 3(*f*), while figures 3(*g*) and (*h*) illustrate contours of L_2^* and the vorticity $\partial L_2^*/\partial Y^*$.

Close to the wall, i.e. as $Y \to 0$,

$$\dot{x} \sim -\tfrac{3}{4}\gamma^2\beta_2^2 xy^2, \quad (\dot{z}, \rho) \sim (\dot{z}_s, \rho_s) - (\dot{\bar{z}}_2, \bar{\rho}_2)\frac{2}{\sqrt{3}}\frac{\beta_0}{\gamma}\frac{1}{y}, \tag{4.14a, b}$$

which match to a regular vorticity layer of similar form to (3.24). Similarly a match can be achieved with a separating layer governed by a Prandtl transformation above the central inviscid region.

Figure 3(*i*) shows the characteristics, i.e. lines of constant x and z, for $\delta t > 0$. Integration of the continuity equation yields a singularity over a segment $-1 < \tilde{Z} < 1$ of the symmetry line $\tilde{X} = 0$. Since neither the singularity nor any particles on the symmetry line leave the symmetry line, the region of inaccessibility remains restricted to the symmetry line.

A special case occurs for separation at the intersection of two symmetry lines, such as at the apex of an ellipsoid. In that case, in addition to the symmetry in ξ, x is an even function of ζ and z an odd one, and the transformations of the Lagrangian coordinate system (4.2) and (4.3) become trivial. No changes in the leading-order singularity structure occur, since it was already symmetric in z-direction, even though this condition was not imposed. However, the velocity parallel to the symmetry plane must be antisymmetric, and the density symmetric, cf. (4.13*b*):

$$\dot{z} \sim |\delta t|^{\frac{1}{2}}\dot{\bar{z}}_3\frac{\beta_2}{\beta_1\bar{z}_3}\tilde{Z}, \quad \rho \sim \rho_s + |\delta t|^{\frac{1}{2}}\bar{\rho}_2\beta_0\beta_2(\tilde{Z}^2+1)^{\frac{1}{2}}L_2^*. \tag{4.15a, b}$$

In the case of two-dimensionality, where x is independent of ζ, the coefficient β_1 vanishes as in the previous subsection, suppressing the decay of the boundary-layer

thickness with z. The flow on the symmetry line can then be written as a one-dimensional problem, and was studied from an Eulerian standpoint by Banks & Zaturska (1979) and Simpson & Stewartson (1982*a*, *b*). In Part 2, Van Dommelen (1989) uses this flow to verify the Lagrangian analysis numerically to high accuracy. Favourable numerical comparisons with the singularity structure away from the symmetry line have been obtained by Lam (1988) for starting flow through a circular pipe.

The existence of this singularity has also been reported by Stern & Paldor (1983), Russell & Landahl (1984) and Stuart (1988) while studying inviscid models for the growth of large-amplitude disturbances in boundary layers. In fact, because unsteady separation is primarily inviscid in its final stages, an alternative approach to that above would be to solve the inviscid version of (2.3) exactly, and then to examine the possible singularities of the solutions (see also Van Dommelen 1981 for the two-dimensional singularity). This is essentially what Stuart (1988) has done in his exact, inviscid, 'stagnation point' analysis. His symmetry assumptions make it possible to solve the inviscid governing equations explicitly in both Eulerian and Lagrangian coordinates. The singularity structure he identifies is equivalent to the above, although the extra symmetry implicit in the stagnation-point assumption leads to (4.15*a*, *b*) rather than (4.13*b*).

As in §3 the above singular solution will not remain valid for sufficiently small $|\delta t|$ because previously neglected pressure gradients will become important (cf. the interactive problem for the two-dimensional singularity formulated by Elliott *et al.* 1983). Further, because the velocity towards the separation line is much smaller in the upper and lower vorticity layers than in the central layer, it is in the vorticity layers that the effect of the pressure gradient will be felt first. However, it is the central layer that is responsible for the growth in boundary-layer thickness; thus it appears that the first asymptotic rescaling does not lead to an 'interactive' effect to smooth out the above singularity. Instead, the singularity continues to be driven by the flow in the central layer, while significant changes occur in the upper and lower layers. Similar arguments seem to hold for the singularities in §§4.3 and 4.4 below.

4.3. *Axisymmetric boundary-layer flow with swirl*

Axisymmetric separation can occur on rotationally symmetric spinning bodies such as a disk (Bodonyi & Stewartson 1977) or a sphere (Van Dommelen 1987) when their sense of rotation is suddenly reversed.

In axisymmetric flow, the flow geometry does not depend on ξ and ζ individually, but only on the Lagrangian distance,

$$\psi = (\xi^2 + \zeta^2)^{\frac{1}{2}}, \tag{4.16}$$

from the axis $\xi = \zeta = 0$. The displacement of rings of particles $\psi = \eta = t =$ constant from their original position must remain restricted to a change in physical distance,

$$r = (x^2 + z^2)^{\frac{1}{2}}, \tag{4.17}$$

from the axis, a rotation around the axis, and a shift in vertical position. Hence according to the theory of orthogonal matrices, the solution must be of the form

$$x = c(\psi^2, \eta, t)\,\xi + s(\psi^2, \eta, t)\,\zeta, \tag{4.18a}$$

$$z = -s(\psi^2, \eta, t)\,\xi + c(\psi^2, \eta, t)\,\zeta, \tag{4.18b}$$

where, because of the assumption of regular x and z,

$$c \sim x_{,\xi}(0,\eta,0,t)+\tfrac{1}{6}x_{,\xi\xi\xi}(0,\eta,0,t)\,\psi^2+\ldots, \tag{4.19a}$$

$$s \sim x_{,\zeta}(0,\eta,0,t)+\tfrac{1}{6}x_{,\zeta\zeta\zeta}(0,\eta,0,t)\,\psi^2+\ldots. \tag{4.19b}$$

In terms of c and s the physical distance from the axis is given by

$$r^2 = (c^2+s^2)\,\psi^2. \tag{4.20}$$

The Jacobian J in (2.2) can be written in terms of ψ and r as

$$J = (r^2)_{,\psi^2}\,y_{,\eta}-(r^2)_{,\eta}\,y_{,\psi^2}. \tag{4.21}$$

The separation occurs at a stationary point for $r^2(\psi^2,\eta,t)$, and from (4.20) and (4.21) it occurs on the axis when

$$c(0,\eta_s,t_s) = s(0,\eta_s,t_s) = 0. \tag{4.22a, b}$$

A rotation of the Lagrangian coordinate system to diagonalize the second-order derivatives of x is not advantageous here, since the axial symmetry would be lost. Instead we rotate the coordinate system around the symmetry axis,

$$\tilde{k}_1 = \frac{x_{23}\,\xi-x_{12}\,\zeta}{(x_{12}^2+x_{23}^2)^{\frac{1}{2}}},\quad \tilde{k}_2 = \eta-\eta_s,\quad \tilde{k}_3 = \frac{x_{12}\,\xi+x_{23}\,\zeta}{(x_{12}^2+x_{23}^2)^{\frac{1}{2}}}, \tag{4.23a–c}$$

to eliminate the $\tilde{x}_{12}$ derivative, followed by the shearing transformation

$$l_1 = \tilde{k}_1,\quad l_2 = \tilde{k}_2+\frac{\tilde{x}_{333}}{6\tilde{x}_{23}}(\tilde{k}_1^2+\tilde{k}_3^2)+\delta t\frac{\dot{\tilde{x}}_3}{\tilde{x}_{23}},\quad l_3 = \tilde{k}_3, \tag{4.24a–c}$$

to eliminate $\bar{x}_{333}$ and $\dot{\tilde{x}}_3$.

The characteristics of the Jacobian are lines of constant distance r from the axis. If t_s is the first time that a singularity forms then $\bar{x}_{111}\dot{\bar{x}}_1$ must be negative, or for a suitable choice of the positive l_1 direction

$$\bar{x}_{111} > 0,\quad \dot{\bar{x}}_1 < 0. \tag{4.25a, b}$$

The characteristic lines of constant r in the (ψ, l_2)-plane appear as sketched in figure 4(*a*), which may be compared to figures 2(*a*) and 3(*a*).

Appropriate local scalings are

$$\psi = |\delta t|^{\frac{1}{2}}\beta\Psi^*,\quad l_2 = |\delta t|\,\beta_0\beta^2 L_2^*,\quad r = |\delta t|^{\frac{3}{2}}\alpha\beta^3 R^*,\quad y = \frac{Y^*}{|\delta t|\,\gamma\beta^2}, \tag{4.26a–d}$$

$$\alpha = \tfrac{1}{3}\bar{x}_{111},\quad \gamma = \tfrac{1}{3}\bar{x}_{111}(\bar{x}_{23}^2)^{\frac{1}{2}}\frac{\rho_s H_s}{\rho_{0s}H_{0s}},\quad \beta_0 = \frac{\bar{x}_{111}}{2(\bar{x}_{23}^2)^{\frac{1}{2}}},\quad \beta = \left(-\frac{2\dot{\bar{x}}_1}{\bar{x}_{111}}\right)^{\frac{1}{2}}, \tag{4.26e–h}$$

leading to a continuity integral

$$Y^* \sim \int_0^{\Psi_0^*}\frac{2\mathrm{d}\Psi^*}{(4R^{*2}-(3\Psi^*+\Psi^{*3})^2)^{\frac{1}{2}}}\pm\int_{\Psi^*}^{\Psi_0^*}\frac{2\mathrm{d}\Psi^*}{(4R^{*2}-(3\Psi^*+\Psi^{*3})^2)^{\frac{1}{2}}}, \tag{4.27a}$$

where

$$\Psi_0^*(R^*) = I(R^*). \tag{4.27b}$$

This can be written as the elliptic integral

$$Y^*(L_2^*,R^*) = \frac{2}{A}F\left(\frac{\pi}{2}\middle|\,m\right)\pm\frac{1}{A}F(\phi\,|\,m), \tag{4.28a}$$

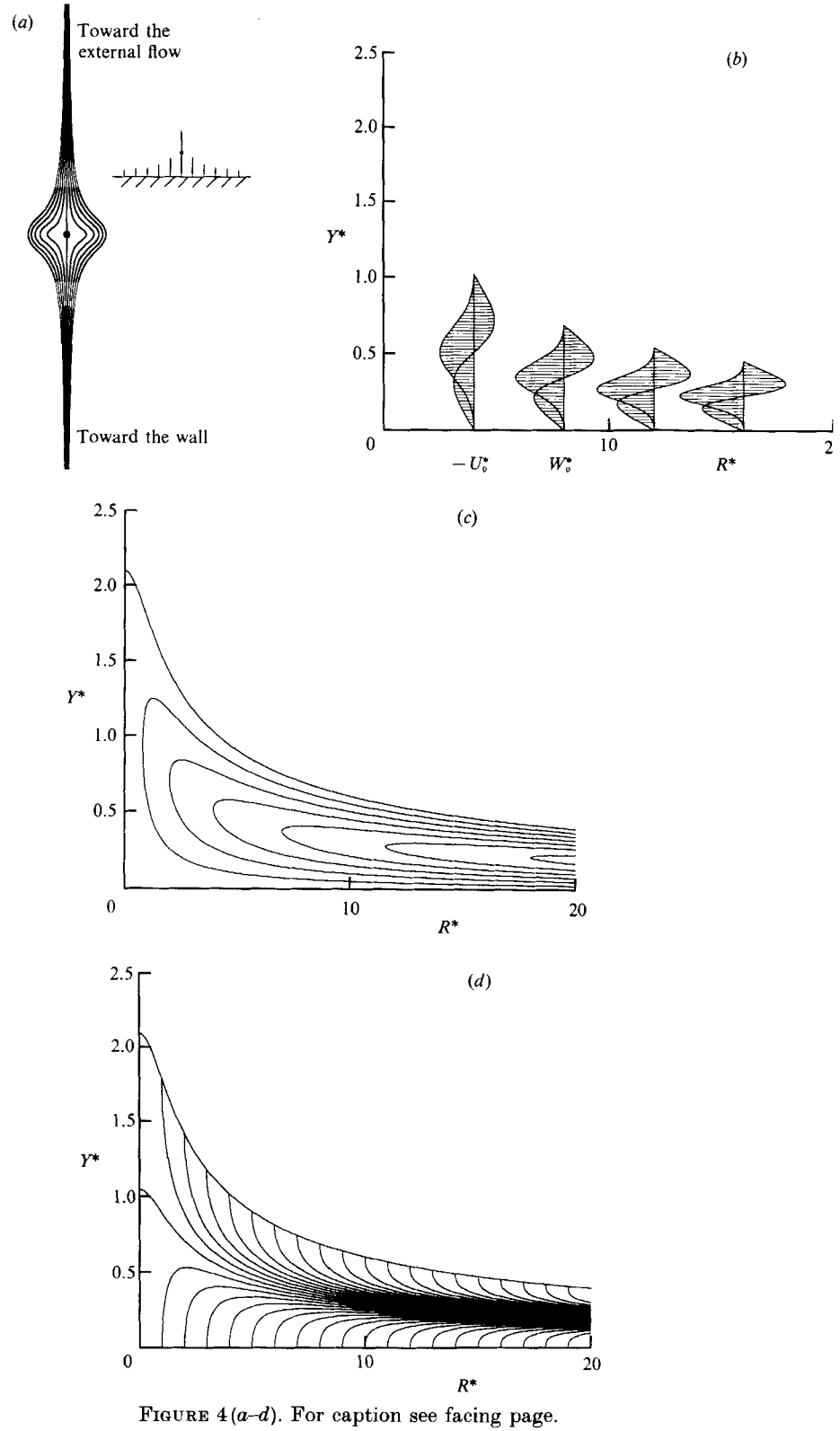

FIGURE 4 (*a–d*). For caption see facing page.

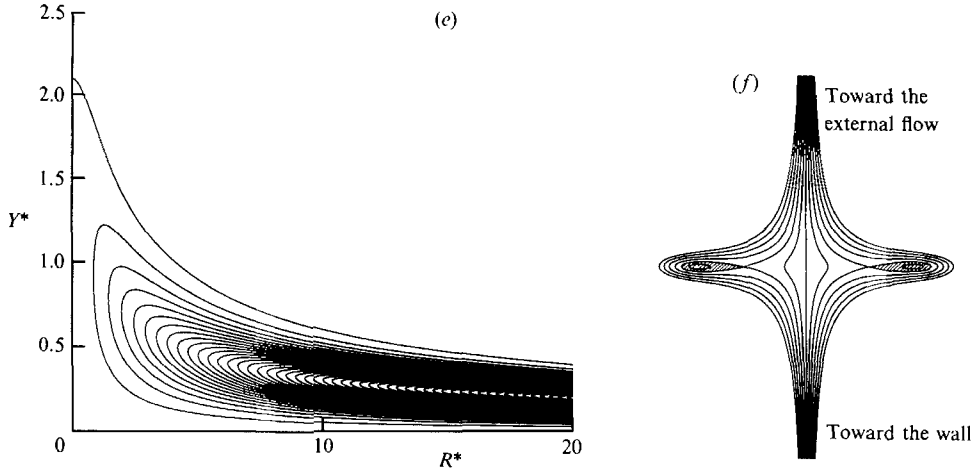

FIGURE 4. Structure of axisymmetric separation with swirl: (*a*) Lagrangian topology of physically vertical lines; (*b*) the velocity profiles of the two components $-U_0^*$ and W_0^*; (*c*) contours of the scaled absolute velocity $\Psi^* = 0, \frac{1}{2}, 1, 1\frac{1}{2}, \ldots$; (*d*) contours of the scaled vorticity component normal to the flow velocity $\Omega_n = 0, \pm 1, \pm 2, \ldots$; (*e*) contours of the scaled vorticity component parallel to the velocity $\Omega_p = 0, -1, -2, \ldots$; (*f*) Lagrangian topology of physically vertical lines beyond the first singularity.

where

$$\Lambda(R^*) = (3(\Psi_0^{*2}+1)(\Psi_0^{*2}+3)^3)^{\frac{1}{4}}, \quad m(R^*) = \frac{1}{2} - \frac{3\Psi_0^{*4}+18\Psi_0^{*2}+18}{4\Lambda^2}, \tag{4.28b, c}$$

$$\phi(L_2^*, R^*) = 2\arctan\left[\frac{1}{\Lambda}\left((\Psi_0^{*2}+3)^2\left(\frac{\Psi_0^{*2}}{\Psi^{*2}}-1\right)\right)^{\frac{1}{3}}\right], \tag{4.28d}$$

and Ψ^{*2} is related to L_2^* and R^* through the solution of the cubic equation

$$4R^{*2} = 9L_2^{*2}\,\Psi^{*2} + (\Psi^{*2}+3)^2\,\Psi^{*2}. \tag{4.28e}$$

On the axis, (4.28*a*) simplifies to

$$Y^*(L_2^*, 0) = \tfrac{2}{3}(\tfrac{1}{2}\pi + \arctan L_2^*), \tag{4.29}$$

while for large R^*, the boundary-layer thickness asymptotes to

$$y^+ \sim \frac{4\alpha^{\frac{2}{3}}}{3^{\frac{1}{3}}2^{\frac{2}{3}}\gamma} F\left(\frac{\pi}{2}\middle|\frac{1}{2}-\frac{\sqrt{3}}{4}\right)\frac{1}{r^{\frac{2}{3}}} \quad \text{for} \quad |\delta t|^{\frac{3}{2}} \ll r \ll 1. \tag{4.30}$$

The velocity components in the radial and azimuthal directions, and the density, are

$$\dot{r} \sim -|\delta t|^{\frac{1}{2}}\tfrac{3}{2}\alpha\beta^3(U_0^* + \chi W_0^*), \quad r\dot{\theta} \sim |\delta t|^{\frac{1}{2}}\tfrac{3}{2}\alpha\beta^3\kappa(W_0^* - \chi U_0^*), \quad \chi = \frac{\kappa\dot{\bar{x}}_3}{\dot{\bar{x}}_1}, \tag{4.31a–c}$$

$$\rho = \rho_s + |\delta t|\,(\bar{\rho}_2\beta_0\beta^2 L_2^* + \tfrac{1}{2}\bar{\rho}_{11}\beta^2\Psi^{*2} - \dot{\bar{\rho}}), \tag{4.31d}$$

where $\kappa = \operatorname{sgn}(\bar{x}_{23})$, and

$$U_0^* = \frac{(\Psi^{*2}+3)\,\Psi^{*2}}{2R^*}, \quad W_0^* = \frac{3\Psi^{*2}L_2^*}{2R^*}, \tag{4.32a, b}$$

are the symmetric and antisymmetric velocity profiles shown in figure 4(*b*). It can be seen from these profiles that the sense of rotation of the fluid about the axis must reverse inside the boundary layer in order for the separation process to be possible. This situation occurs when the direction of rotation of a spinning body is reversed. What happens when the spin is brought to a halt instead is not clear (Van Dommelen 1987).

Both the radial and the circumferential velocity profiles depend non-trivially on the parameter χ. However the magnitude of the velocity,

$$q = (u^2+w^2)^{\frac{1}{2}} = |\delta t|^{\frac{1}{2}}\tfrac{3}{2}\alpha\beta^3(1+\chi^2)^{\frac{1}{2}}\,\Psi^*, \tag{4.33}$$

does not; contours of q are illustrated in figure 4(*c*). The vorticity components normal to the velocity and parallel to it are proportional to

$$\Omega_{\mathrm{n}} = \frac{U_0^*\,U_{0Y^*}^* + W_0^*\,W_{0Y^*}^*}{(U_0^{*2}+W_0^{*2})^{\frac{1}{2}}} = -\tfrac{3}{2}\Psi^* L_2^*, \tag{4.34a, b}$$

$$\Omega_{\mathrm{p}} = \frac{W_0^*\,U_{0Y^*}^* - U_0^*\,W_{0Y^*}^*}{(U_0^{*2}+W_0^{*2})^{\frac{1}{2}}} = -\tfrac{3}{2}\Psi^*(\Psi^{*2}+1). \tag{4.35a, b}$$

Contours of these quantities are plotted in figures 4(*d*) and 4(*e*) respectively.

A match with the sandwich layer adjacent to the wall is again possible, since as $Y \to 0$

$$\dot{r} \sim \tfrac{3}{2}\gamma\beta^2\chi r y, \quad r\dot{\theta} \sim -\tfrac{3}{2}\gamma\beta^2\kappa r y, \quad \rho \sim \rho_{\mathrm{s}} - \bar{\rho}_2\frac{2}{3}\frac{\beta_0}{\gamma}\frac{1}{y}. \tag{4.36a–c}$$

Similarly a match can be achieved with the upper separating layer.

Figure 4(*f*) shows the characteristics for $\delta t > 0$. The singular line is the physically expanding circle $R^* = 1$, but the region of inaccessibility is larger owing to particles with $L_2^* \neq 0$ which move radially outward from the singular line at a greater rate.

On the axis itself, the continuity integral is particularly simple:

$$y = \int_0^{\eta} \frac{\rho_0 H_0\,\mathrm{d}\eta}{\rho H (x_{,\xi})^2 + (x_{,\xi})^2}. \tag{4.37}$$

When this integral is expanded to second order, a logarithmic correction to the y-position is obtained. This and other terms were initially overlooked in Eulerian analyses of the flow on the axis (Bodonyi & Stewartson 1977; Banks & Zaturska 1981), but in a Lagrangian approach the logarithmic term follows naturally from the hypothesis that the solution for the motion parallel to the boundary is regular. (A similar logarithmic term arises in the symmetric case, §4.2 above, cf. Part 2.) In fact, from this hypothesis alone, the complete singularity structure presented by Stewartson *et al.* (1982) can be recovered by means of a simple integration of (4.37).

4.4. *Axisymmetric boundary-layer collision without swirl*

Finally, we consider the case of axially symmetric flow when there is no rotation of the flow about the axis. This case is of interest for heated axially symmetric bodies when the axis is vertical (Brown & Simpson 1982; Awang & Riley 1983), and might occur in other axially symmetric flows in which the fluid is driven toward the axis.

In the absence of rotation (4.18) simplifies to

$$x = c(\psi^2, \eta, t)\,\xi, \quad z = c(\psi^2, \eta, t)\,\zeta. \tag{4.38}$$

No transformations of the Lagrangian coordinate system are needed in this case. It follows that if a singularity first appears on the axis c must vanish. The contours of constant r are then identical to those for a symmetric collision (figure 3a), while the Taylor series coefficients satisfy conditions (4.6a, b, d).

In a similar way to before, suitable local scalings are

$$\psi = |\delta t|^{\frac{1}{2}}\beta\Psi^*, \quad l_2 = |\delta t|^{\frac{1}{2}}\beta_0\beta L_2^*, \quad r = |\delta t|^{\frac{3}{2}}\alpha\beta^3 R^*, \quad y = \frac{Y^*}{|\delta t|^{\frac{3}{2}}\gamma\beta^3}, \tag{4.39a–d}$$

$$\alpha = \tfrac{1}{3}\bar{x}_{111}, \quad \gamma = \tfrac{1}{3}(\tfrac{1}{3}\bar{x}_{111}^3\,\bar{x}_{122})^{\frac{1}{2}}\frac{\rho_s H_s}{\rho_{0s} H_{0s}}, \quad \beta_0 = \left(\frac{\bar{x}_{111}}{\bar{x}_{122}}\right)^{\frac{1}{2}}, \quad \beta = \left(-\frac{2\dot{\bar{x}}_1}{\bar{x}_{111}}\right)^{\frac{1}{2}}, \tag{4.39e–h}$$

leading to a continuity integral

$$Y^* \sim \int_0^{\Psi_0^*} \frac{\Psi^{*\frac{1}{2}}\,\mathrm{d}\Psi^*}{R^*(2R^* - 3\Psi^* - \Psi^{*3})^{\frac{1}{2}}} \pm \int_{\Psi^*}^{\Psi_0^*} \frac{\Psi^{*\frac{1}{2}}\,\mathrm{d}\Psi^*}{R^*(2R^* - 3\Psi^* - \Psi^{*3})^{\frac{1}{2}}}, \tag{4.40a}$$

where

$$\Psi_0^*(R^*) = I(R^*). \tag{4.40b}$$

This solution can be 'reduced' to the form

$$\begin{aligned} Y^*(L_2^*, R^*) = {} & \frac{1}{\Psi_0^{*2}+3}\left(\frac{4-4\mathrm{n}}{\Lambda}\Pi(\mathrm{n}\,;\tfrac{1}{2}\pi\,|\,m) - \frac{2}{\Lambda}F(\tfrac{1}{2}\pi\,|\,m)\right) \\ & \pm \frac{1}{\Psi_0^{*2}+3}\left(\frac{2-2\mathrm{n}}{\Lambda}\Pi(\mathrm{n}\,;\phi\,|\,m) - \frac{1}{\Lambda}F(\phi\,|\,m) + \frac{2}{\Psi_0^*}\arctan\left(\frac{\Psi_0^*}{2\Lambda}\frac{\sin(\phi)}{(1-m\sin^2\phi)^{\frac{1}{2}}}\right)\right. \\ & \left. + \frac{2}{\Psi_0^*}\arctan\left(\frac{\mathrm{n}\Psi_0^*}{2\Lambda}\frac{\sin(2\phi)}{(1-m\sin^2\phi)^{\frac{1}{2}}}\right)\right), \end{aligned} \tag{4.41a}$$

where $\Pi(\mathrm{n}\,;\phi\,|\,m)$ is the incomplete elliptic integral of the third kind, and

$$\Lambda(R^*) = (3(\Psi_0^{*2}+1)(\Psi_0^{*2}+3))^{\frac{1}{4}}, \quad m(R^*) = \frac{1}{2} - \frac{3\Psi_0^{*2}+6}{4\Lambda^2}, \quad \mathrm{n}(R^*) = 1 - \frac{3\Psi_0^{*2}+12}{2\Lambda^2+6}, \tag{4.41b–d}$$

$$\phi(L_2^*, R^*) = 2\arctan\left[\frac{1}{\Lambda}\left((\Psi_0^{*2}+3)\left(\frac{\Psi_0^*}{\Psi^*}-1\right)\right)^{\frac{1}{2}}\right], \tag{4.41e}$$

$$\Psi^*(L_2^*, R^*) = (L_2^{*2}+1)^{\frac{1}{2}} I(R^*/(L_2^{*2}+1)^{\frac{3}{2}}). \tag{4.41f}$$

On the axis (4.41a) simplifies to

$$Y^*(L_2^*, 0) = \frac{2}{3\sqrt{3}}\left(\tfrac{1}{2}\pi + \arctan L_2^* + \frac{L_2^*}{L_2^{*2}+1}\right), \tag{4.42}$$

while for large R^* the boundary-layer thickness asymptotes to

$$y^+ \sim \frac{2\alpha}{3^{\frac{1}{4}}\gamma}\left(\sqrt{3}\Pi\left(1 - \frac{\sqrt{3}}{2}; \frac{\pi}{2}\middle|\frac{1}{2} - \frac{\sqrt{3}}{4}\right) - F\left(\frac{\pi}{2}\middle|\frac{1}{2} - \frac{\sqrt{3}}{4}\right)\right)\frac{1}{r}. \tag{4.43}$$

The velocity and density are given to leading order by

$$\dot{r} \sim -|\delta t|^{\frac{1}{2}}\tfrac{3}{2}\alpha\beta^3\Psi^*, \quad \rho \sim \rho_s + |\delta t|^{\frac{1}{2}}\bar{\rho}_2\beta_0\beta L_2^*. \tag{4.44a, b}$$

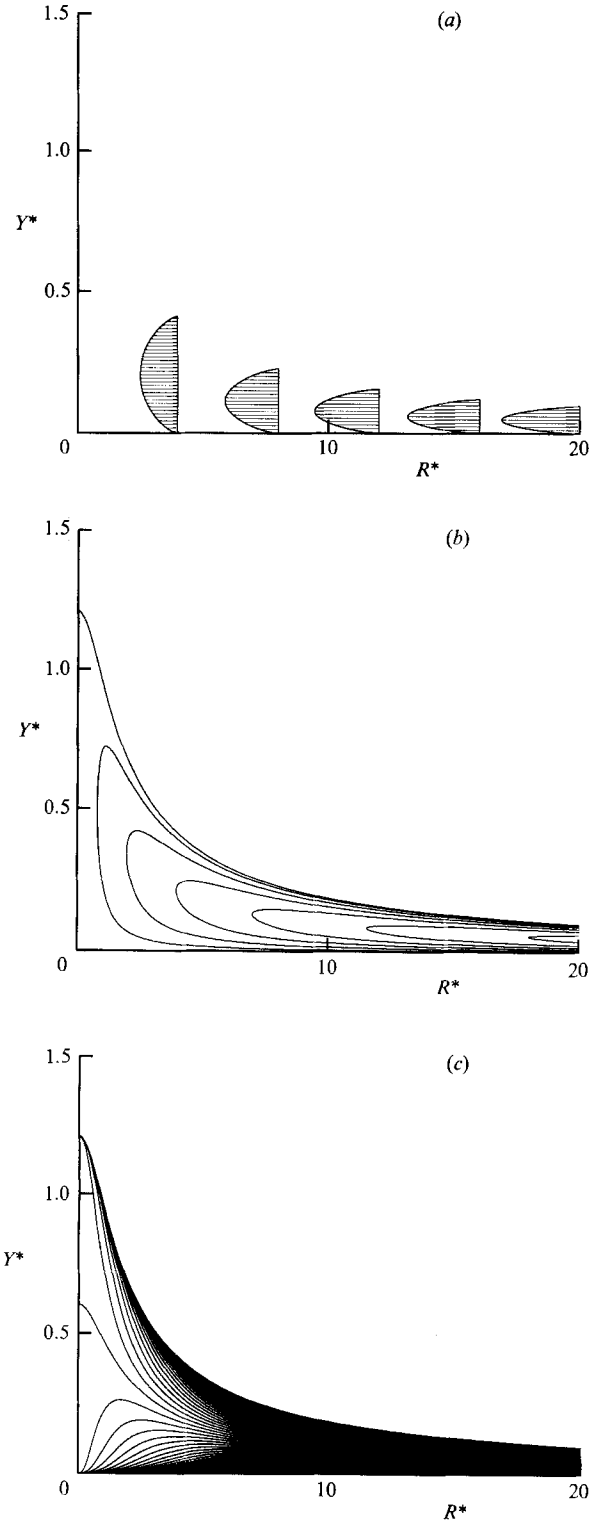

FIGURE 5. Structure of axisymmetric separation without swirl: (*a*) Ψ^* velocity profiles; (*b*) contours of $\Psi^* = 0, \frac{1}{2}, 1, 1\frac{1}{2}, \ldots$; (*c*) contours of $\partial P^*/\partial Y^* = 0, \pm 1, \pm 2, \ldots$.

Sample velocity profiles are illustrated in figure 5(*a*). The velocity must have a minimum inside the boundary layer for this separation process to be possible. Contours of Ψ^* and the vorticity $\partial\Psi^*/\partial Y^*$ are given in figures 5(*b*) and 5(*c*) respectively. Again, a match is possible with the wall layer, since as $Y \to 0$,

$$\dot{r} \sim -\frac{3^{\frac{5}{3}}}{2^{\frac{4}{3}}}\beta^2\gamma^{\frac{2}{3}}ry^{\frac{2}{3}}, \quad \rho \sim \rho_s + \bar{\rho}_2\frac{2^{\frac{2}{3}}\beta_0}{3^{\frac{5}{6}}}\frac{1}{\gamma^{\frac{1}{3}}}\frac{1}{y^{\frac{1}{3}}}. \tag{4.45a, b}$$

5. Discussion

In this paper we have shown that the description of attached flow past a body using the classical boundary-layer equations can break down after a finite time owing to the formation of a local singularity. In a Lagrangian description the class of singularities is characterized by a singular continuity equation, but a regular momentum equation. The evidence shows that such singularities are both mathematically consistent and physically relevant (e.g. Bouard & Coutanceau 1980; Van Dommelen & Shen 1980*a*; Van Dommelen 1987, 1989; Lam 1988). The precise structure of the singularity depends on the symmetry of the flow, and some of the simpler structures have previously been partially or totally described in Eulerian coordinates by other authors. The purpose of this paper is to provide a unified theory to facilitate the identification of singularities of the Lagrangian type when they do occur. This seems especially relevant for the difficult problem of the asymmetric singularity, where the singular behaviour would have to be deduced from a three-dimensional unsteady computation.

These singularities occur when a fluid particle becomes compressed in one direction parallel to the boundary. Conservation of mass then implies that fluid above this fluid particle is forced out of the boundary layer in the form of a detached vorticity layer. A common feature of all the singularities is that the typical lengthscale in the direction of compression is $O(|\delta t|^{\frac{3}{2}})$. However, the strength of the singularity increases with the symmetry of the flow; the boundary-layer thickness varies from $O(|\delta t|^{-\frac{1}{4}})$ for the asymmetric singularity to $O(|\delta t|^{-\frac{3}{2}})$ for the axisymmetric singularity without swirl.

Because the singularities take the form of a vertical ejection of fluid from the boundary layer, we believe that they indicate the onset of separation as hypothesized by Sears & Telionis (1975). While the present singularity structures do at least seem to describe the initial genesis of the separating shear layer, within an asymptotically short time interactive effects which are neglected in the classical boundary-layer formulation must be included (e.g. Elliott *et al.* 1983; Henkes & Veldman 1987). At that stage a new asymptotic scaling must be substituted into the Navier–Stokes equations in order to recover the correct large-Reynolds-number limit. Knowledge of the precise asymptotic structure of the singularities is necessary to identify this new scaling, and one of the contributions of this work has been to identify the full structure of a number of symmetric singularities.

At first sight the symmetric singularities may appear less likely to occur in problems of practical importance. However, they have previously arisen in inviscid models of 'transition to turbulence' in regions where symmetric counter-rotating longitudinal vortices are forcing the convergence of fluid particles (Stern & Paldor 1983; Russell & Landahl 1984; Stuart 1988). A three-dimensional extension of the work by Smith & Burggraf (1985) may lead to an asymptotic description of transition which accounts for viscosity, where the turbulent bursts are associated with local regions of classical boundary-layer separation (symmetric or otherwise).

This work was presented in part at the IUTAM 'Fluid Mechanics in the Spirit of G. I. Taylor' Conference, April 1986, Cambridge. The authors acknowledge financial support from the NASA 'Materials Processing in Space' program, the SERC, the AFOSR, and ICOMP, NASA Lewis.

REFERENCES

AWANG, M. A. O. & RILEY, N. 1983 Unsteady free convection from a heated sphere at high Grashof number. *J. Engng Maths* **17**, 355–365.

BANKS, W. H. H. & ZATURSKA, M. B. 1979 The collision of unsteady laminar boundary layers. *J. Engng Maths* **13**, 193–212.

BANKS, W. H. H. & ZATURSKA, M. B. 1981 The unsteady boundary-layer development on a rotating disc in counter rotating flow. *Acta Mech.* **38**, 143–155.

BLASIUS, H. 1908 Grenzschichten in Flussigkeiten mit kleiner Reibung. *Z. Math. Phys.* **56**, 1–37.

BODONYI, R. J. & STEWARTSON, K. 1977 The unsteady laminar boundary layer on a rotating disk in a counter-rotating fluid. *J. Fluid Mech.* **79**, 669–688.

BOUARD, R. & COUTANCEAU, M. 1980 The early stage of development of the wake behind an impulsively started cylinder for $40 < Re < 10000$. *J. Fluid Mech.* **101**, 583–607.

BROWN, S. N. 1965 Singularities associated with separating boundary layers. *Phil. Trans. R. Soc. Lond.* A **257**, 409–444.

BROWN, S. N. & SIMPSON, C. J. 1982 Collision phenomena in free-convective flow over a sphere. *J. Fluid Mech.* **124**, 123–127.

CEBECI, T. 1982 Unsteady separation. In *Numerical and Physical Aspects of Aerodynamic Flows* (ed. T. Cebeci), pp. 265–277. Springer.

CEBECI, T. 1986 Unsteady boundary layers with an intelligent numerical scheme. *J. Fluid Mech.* **163**, 129–140.

CEBECI, T., KHATTAB, A. K. & SCHIMKE, S. M. 1983 Can the singularity be removed in time-dependent flows? In *Proc. A.F. Workshop, Colorado Springs.*

CEBECI, T., KHATTAB, A. K. & STEWARTSON, K. 1981 Three-dimensional boundary layers and the ok of accessibility. *J. Fluid Mech.* **107**, 57–87.

CEBECI, T., STEWARTSON, K. & SCHIMKE, S. M. 1984 Unsteady boundary layers close to the stagnation region of slender bodies. *J. Fluid Mech.* **147**, 315–332.

COWLEY, S. J. 1983 Computer extension and analytic continuation of Blasius' expansion for impulsive flow past a circular cylinder. *J. Fluid Mech.* **135**, 389–405.

DIDDEN, N. & HO, C.-M. 1985 Unsteady separation in a boundary layer produced by an impinging jet. *J. Fluid Mech.* **160**, 235–256.

ECE, M. C., WALKER, J. D. A. & DOLIGALSKI, T. L. 1984 The boundary layer on an impulsively started rotating and translating cylinder. *Phys. Fluids* **27**, 1077–1089.

ELLIOTT, J. W., COWLEY, S. J. & SMITH, F. T. 1983 Breakdown of boundary layers:, i. on moving surfaces, ii. in semi-similar unsteady flow, iii. in fully unsteady flow. *Geophys. Astrophys. Fluid Dyn.* **25**, 77–138.

GOLDSTEIN, S. 1948 On laminar boundary-layer flow near a position of separation. *Q. J. Mech. Appl. Maths* **1**, 43–69.

HENKES, R. A. W. M. & VELDMAN, A. E. P. 1987 On the breakdown of the steady and unsteady interacting boundary-layer description. *J. Fluid Mech.* **179**, 513–530.

HUDSON, J. A. 1980 *The Excitation and Propagation of Elastic Waves.* Cambridge University Press.

INGHAM, D. B. 1984 Unsteady separation. *J. Comput. Phys.* **53**, 90–99.

LAM, S. T. 1988 On high-Reynolds-number laminar flows through a curved pipe, and past a rotating cylinder. Ph.D. dissertation, University of London.

LAMB, H. 1945 *Hydrodynamics.* Dover.

LUDWIG, G. R. 1964 An experimental investigation of laminar separation from a moving wall. *AIAA Paper* 64–6.

MATSUSHITA, M., MURATA, S. & AKAMATSU, T. 1984 Studies on boundary-layer separation in unsteady flow using an integral method. *J. Fluid Mech.* **149**, 477–501.

McCroskey, W. J. & Pucci, S. L. 1982 Viscous-inviscid interaction on oscillating airfoils in subsonic flow. *AIAA J.* **20**, 167–174.

Moore, F. K. 1958 On the separation of the unsteady laminar boundary layer. In *Boundary-Layer Research* (ed. H. G. Görtler), pp. 296–311. Springer.

Nagata, H., Minami, K. & Murata, Y. 1979 Initial flow past an impulsively started circular cylinder. *Bull. JSME* **22**, 512–520.

Ockendon, H. 1972 An asymptotic solution of steady flow above an infinite rotating disk with suction. *Q. J. Mech. Appl. Maths* **25**, 291–301.

Prandtl, L. 1904 Uber Flüssigkeitsbewegung bei sehr kleiner Reibung. In *Ludwig Prandtl gesammelte Abhandlüngen*, pp. 575–584. Springer, 1961.

Ragab, S. A. 1986 The laminar boundary layer on a prolate spheroid started impulsively from rest at high incidence. *AIAA Paper* 86–1109.

Rosenhead, L. 1963 *Laminar Boundary Layers*. Oxford University Press.

Rott, N. 1956 Unsteady viscous flows in the vicinity of a separation point. *Q. Appl. Maths* **13**, 444–451.

Russell, J. M. & Landahl, M. T. 1984 The evolution of a flat eddy near a wall in an inviscid shear flow. *Phys. Fluids* **27**, 557–570.

Sears, W. R. 1956 Some recent developments in airfoil theory. *J. Aeronaut. Sci.* **23**, 490–499.

Sears, W. R. & Telionis, D. P. 1975 Boundary-layer separation in unsteady flow. *SIAM J. Appl. Maths* **23**, 215–234.

Shen, S. F. 1978*a* Unsteady separation according to the boundary-layer equation. *Adv. Appl. Mech.* **13**, 177–220.

Shen, S. F. 1978*b* Unsteady separation of three-dimensional boundary layers from the Lagrangian viewpoint. In *Nonsteady Fluid Dynamics* (ed. D. E. Crow & J. A. Miller), pp. 47–51. ASME.

Shen, S. F. & Wu, T. 1988 Unsteady separation over maneuvering bodies. *AIAA Paper* 88-3552-CP.

Simpson, C. J. & Stewartson, K. 1982*a* A note on a boundary-layer collision on a rotating sphere. *Z. Angew. Math. Phys.* **33**, 370–378.

Simpson, C. J. & Stewartson, K. 1982*b* A singularity in an unsteady free-convection boundary layer. *Q. J. Mech. Appl. Maths* **35**, 291–304.

Smith, F. T. 1978 Three-dimensional viscous and inviscid separation of a vortex sheet from a smooth non-slender body. *RAE Tech. Rep.* 78095.

Smith, F. T. 1987 Break-up in unsteady separation. In *Forum on Unsteady Flow Separation*, ASME FED-Vol. 52, pp. 55–64.

Smith, F. T. & Burggraf, O. R. 1985 On the development of large-sized short-scaled disturbances in boundary layers. *Proc. R. Soc. Lond.* A **399**, 25–55.

Stern, M. E. & Paldor, N. 1983 Large amplitude long waves in a shear flow. *Phys. Fluids* **26**, 906–919.

Stewartson, K., Simpson, C. J. & Bodonyi, R. J. 1982 The unsteady boundary layer on a rotating disk in a counter rotating fluid. Part 2. *J. Fluid Mech.* **121**, 507–515.

Stuart, J. T. 1988 Nonlinear Euler partial differential equations: singularities in their solution. In *Proc. Symp. Honor of C. C. Lin* (ed. D. J. Benney, Chi Yuan & F. H. Shu), pp. 81–95. World Scientific.

Sychev, V. V. 1979 Asymptotic theory of non-stationary separation. *Izv. Akad. Nauk. SSSR, Mekh. Zhid. i Gaza* No. 6, 21–32. Also *Fluid Dyn.* **14**, 829–838.

Sychev, V. V. 1980 On certain singularities in solutions of equations of boundary layer on a moving surface. *Prikl. Math. Mech.* **44**, 830–838.

Telionis, D. P. & Tsahalis, D. Th. 1974 Unsteady laminar separation over impulsively moved cylinders. *Acta Astronaut.* **1**, 1487–1505.

Van Dommelen, L. L. 1981 Unsteady boundary-layer separation. Ph.D. dissertation, Cornell University.

Van Dommelen, L. L. 1987 Computation of unsteady separation using Lagrangian procedures. In *Proc. IUTAM Symp. on Boundary-Layer Separation* (ed. F. T. Smith & S. N. Brown), pp. 73–87. Springer.

VAN DOMMELEN, L. L. 1989 On the Lagrangian description of unsteady boundary-layer separation. Part 2. The spinning sphere. *J. Fluid Mech.* **210**, 627–645.

VAN DOMMELEN, L. L. & SHEN, S. F. 1977 Presented at *XIIIth Symp. Bienn. Symp. Adv. Meth. Prob. Fluid Mech., Olsztyn-Kortewo, Poland.*

VAN DOMMELEN, L. L. & SHEN, S. F. 1980*a* The spontaneous generation of the singularity in a separating laminar boundary layer. *J. Comput. Phys.* **38**, 125–140.

VAN DOMMELEN, L. L. & SHEN, S. F. 1980*b* The birth of separation. Presented at the *XVth Intl Congl Theo. Appl. Mech., Toronto, Canada.* IUTAM.

VAN DOMMELEN, L. L. & SHEN, S. F. 1982 The genesis of separation. In *Numerical and Physical Aspects of Aerodynamic Flows* (ed. T. Cebeci), pp. 293–311. Springer.

VAN DOMMELEN, L. L. & SHEN, S. F. 1983*a* Boundary-layer separation singularities for an upstream moving wall. *Acta Mech.* **49**, 241–254.

VAN DOMMELEN, L. L. & SHEN, S. F. 1983*b* An unsteady interactive separation process. *AIAA J.* **21**, 358–362.

VAN DYKE, 1975 *Perturbation Methods in Fluid Mechanics*, p. 86. Stanford: Parabolic.

VASANTHA, R. & RILEY, N. 1988 On the initiation of jets in oscillatory viscous flows. *Proc. R. Soc. Lond.* A **419**, 363–378.

WALKER, J. D. A. 1988 Mechanism of turbulence production near a wall. *ICOMP seminar series, NASA-Lewis, July 26.*

WANG, K. C. 1979 Unsteady boundary-layer separation. *Tech. Rept.* MML TR 79-16c. Baltimore: Martin Marietta Lab.

WANG, K. C. & FAN, Z. Q. 1982 Unsteady symmetry-plane boundary layers and three-dimensional unsteady separation. Part I. High incidence. *San Diego State Univ. Tech. Rep.* AE&EM TR-82-01.

WILLIAMS, J. C. 1977 Incompressible boundary-layer separation. *Ann. Rev. Fluid Mech.* **9**, 113–144.

WILLIAMS, J. C. 1978 On the nature of unsteady three-dimensional laminar boundary-layer separation. *J. Fluid Mech.* **88**, 241–258.

WILLIAMS, J. C. & STEWARTSON, K. 1983 Flow development in the vicinity of the trailing edge on bodies impulsively set into motion. Part 2. *J. Fluid Mech.* **131**, 177.

WU, T. 1989 Ph.D. dissertation, Cornell University.